Assessment of rock glaciers and their water storage in Guokalariju, Tibetan Plateau

~~Assessment of rock glaciers, water storage, and permafrost distribution in Guokalariju, Tibetan Plateau~~

Mengzhen Li, Yanmin Yang, Zhaoyu Peng, Gengnian Liu

College of Urban and Environmental Sciences, Peking University, Beijing, 100871, China

Correspondence to: Gengnian Liu (liugn@pku.edu.cn)

Abstract. Rock glaciers are important hydrological reserves in arid and semi-arid regions. Rock glaciers' activity states can indicate the existence of permafrost. To help explore further the development mechanisms of rock glaciers in semi-arid and humid transition regions, this paper provides a detailed rock glacier inventory of the Guokalariju (GKLRJ) area of the Tibetan Plateau (TP) using a manual visual interpretation of Google Earth Pro remote sensing imagery. We also estimated the water volume equivalent (WVEQ) ~~and the distribution of permafrost probabilities~~ in the GKLRJ for the first time. Approximately 5,~~053~~ 057 rock glaciers were identified, covering a total area of ~~~~404.69~~428.71 km^2. Rock glaciers are unevenly distributed within the three sub-regions R1, R2 and R3 from east to west, with 80% of them concentrated in R2, where climatic and topographic conditions are most favorable. ~~Limited by topographic conditions, rock glaciers are more commonly distributed on west-facing aspects (NW and W).~~ Under the same ground temperature conditions~~When other conditions are met~~, increases in precipitation are conducive to rock glaciers forming at lower altitudes. Indeed, the lower limit of rock glaciers' mean altitude decreased eastward, with increasing precipitation. Estimates of the water storage capacity of rock glaciers obtained by applying different methods varied considerably, but all showed the potential hydrological value of rock glaciers. The maximum possible water storage in the subsurface ice of rock glacier permafrost ~~these rock glaciers~~ was ~~6.82~~3.04 km^3, which is ~~or about ~~ ~~56~~33% of the surface ice in local ~~clean ice~~ glacier storage. In R1, where the climate is the driest, the water storage capacity of rock glaciers was estimated to be up to twice as large as that of the sub-region's ~~clean ice glaciers~~glaciers. Changes in water resources and permafrost stability in the area where rock glaciers distributed will have implications for regional water resource management, disaster prevention, and sustainable development strategies. ~~Permafrost is widespread above ~ 4,476 m above sea level (asl). Our results showed that the regression model, based on the rock glacier inventory, can consistently predict the possible range of modern permafrost. These results may also have some value for regional water resource management, disaster prevention, and sustainable development strategies.~~

1 Introduction

Rock glaciers are periglacial landforms often observed above the timberline in alpine mountains. They are formed by rocks and ice that move down a slope, driven by gravity (French, 2007; RGIK, ~~2021~~2022a). As striking features of viscous flow in perennially frozen materials, they can reflect permafrost conditions in

mountainous areas. Their lowest altitudes are often considered to represent the lower limit of discontinuous regional permafrost occurrence (Giardino and Vitek, 1988; Barsch, 1992, 1996; ~~Barsch, 1996;~~ Kääb ~~et al.~~et al., 1997; Schmid ~~et al.~~et al., 2015; Selley ~~et al.~~et al., 2018; Baral ~~et al.~~et al., 2019; Hassan ~~et al.~~et al., 2021); their states (~~intact~~ active or relict) can be used in Permafrost Zonation Index (PZI) models to predict the probability of permafrost occurrence where field observation data are scarce (Cao ~~et al.~~et al., 2021; Boeckli ~~et al.~~et al., 2012a). The large-scale distribution of active rock glaciers is influenced by the complex interaction of climatic and topographic factors (Schrott, 1996; Millar and Westfall, 2008; Pandey, 2019). Global climate change may affect the stability of rock glaciers and permafrost, thus impacting slope stability, ~~vegetation coverage,~~ runoff patterns and water quality, with possible consequences for periodic landslides, debris flows, floods and other geological disasters (Barsch, 1996; Schoeneich ~~et al.~~et al., 2015; Blöthe ~~et al.~~et al.,2019; Hassan ~~et al.~~et al., 2021). Exploring their spatial distribution and evolution is therefore significant for paleoclimatic modeling, disaster risk assessment and infrastructure maintenance (Arenson and Jakob, 2010; Colucci ~~et al.~~et al., 2016; Selley ~~et al.~~et al., 2018; Alcalá-Reygosa, 2019). Furthermore, the slow thawing process through heat diffusion with latent heat exchange at depth, combined with the cooling effect of the ventilated coarse blocks at the surface of rock glaciers, make them a largely inert hydrological reserve in high mountain systems (Bolch and Marchenko, 2009; Berthling, 2011; Bonnaventure and Lamoureux, 2013; Millar and Westfall, 2013). The presence and abundance of rock glaciers can therefore affect the quantities and properties of runoff from high mountain watersheds over extended time periods (~~Bosson and Lambiel, 2016;~~ Jones ~~et al.~~et al., 2019b).

The Tibetan Plateau (TP) is among the key high-altitude areas of periglacial landform worldwide, and is a region highly sensitive to climate change (Cui ~~et al.~~et al., 2019; Yao ~~et al.~~et al., 2019). Detailed rock glacier inventories have previously been constructed for the Gangdise Mountains (Zhang ~~et al.~~et al., 2022), the Daxue Mountains (Ran and Liu, 2018), the Nyainqêntanglha Range (Reinosch ~~et al.~~et al., 2021), and the Nepalese Himalaya (Jones ~~et al.~~et al., 2018b). The Yarlung Zangbo River Basin (YZRB) is one of the regions with the highest concentrations of modern glaciers on the TP; it is experiencing ~~the most~~ rapid geomorphic evolution ~~on Earth~~ today (Ji ~~et al.~~et al., 1999; Korup and Montgomery, 2008; Yu ~~et al.~~et al., 2011; Long ~~et al.~~et al., 2022). Although Guo (2019) characterized the spatial distribution of rock glaciers in the YZRB using manual visual interpretation, there remains a lack of any systematic and detailed rock glacier inventory, and the regional occurrence characteristics and indicative environmental significance of these rock glaciers are still unclear. Even though ground-penetrating radar (GPR), seismic refraction tomography (SRT), electrical resistivity tomography (ERT) and other geophysical techniques are widely used today and can provide new insights into understanding the ice volumes of rock glaciers and permafrost (Janke ~~et al.~~et al., 2015; Emmert and Kneisel, 2017; Bolch ~~et al.~~et al., 2019; Buckel ~~et al.~~et al., 2021; Halla ~~et al.~~et al., 2021; Mathys ~~et al.~~et al., 2022), it remains ~~problematic~~ difficult to apply such methods to large-scale field-based research on the TP. The distribution of permafrost and the hydrological contributions made by rock glaciers on the TP need more research.

To address this, our study aims to: (i) compile a more comprehensive and systematic inventory of rock glaciers in the GLKRJ; (ii) explore the regional occurrence characteristics and indicative environmental significance of these rock glaciers; (iii) assess the regional hydrological significance of rock glaciers and ~~clean ice glaciers~~glaciers; and (iv) ~~model~~ compare the distribution of the GLKRJ's rock glaciers to the regional permafrost maps~~permafrost probabilities~~.

2 Study area

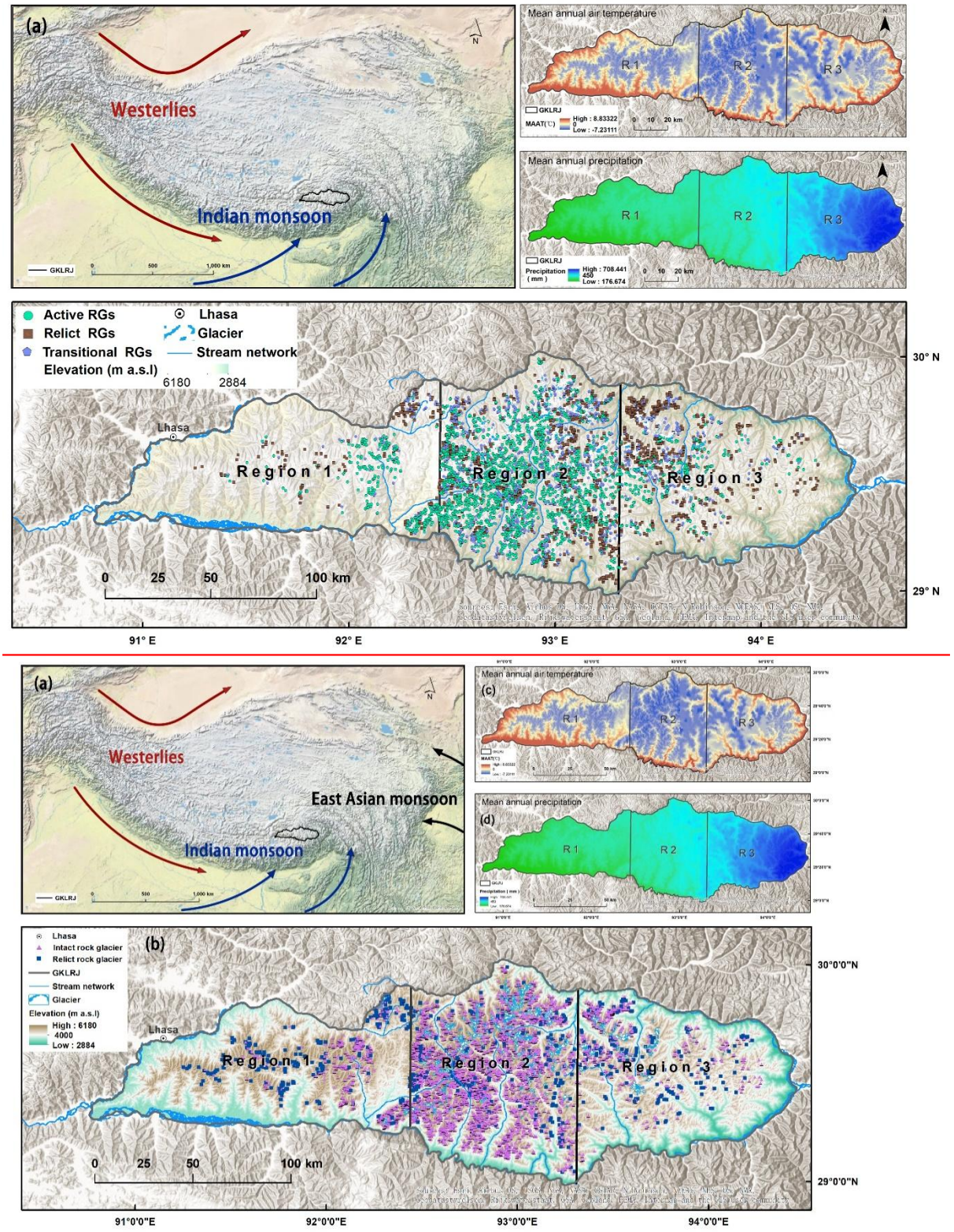

Figure 1: (a) The location of the GKLRJ on the TP; (b) The three sub-regions and the spatial distribution of streams. Rock glaciers are categorized as green (active rock glaciers), purple (transitional~~intact~~ rock glaciers), brown~~blue~~ (relict rock glaciers), and glaciers are shown in light blue and white; (c) Mean annual air temperature map for the GKLRJ (Du and Yi, 2019); (d) Mean annual precipitation map for the GKLRJ (Du and Yi, 2019). Maps were created using ArcGIS® software by Esri.

The GKLRJ region is located between 92.916°N – -93.276°N and 29.287°E – -29.438°E, on the

southeastern TP, adjacent to the Himalayas to the south and the Nyainqêntanglha Range to the north (see Fig.1). It forms the eastern extension of the Gangdise Mountains as well as the watershed of the Yarlung Zangbo River and its tributary, the Niyang-Lhasa River, and belongs to the high mountain plateau-lake basin-wide valley area of the middle and upper reaches of the Yarlung Zangbo and Nujiang rivers (Xiang ~~*et al.*~~*et al.*, 2013). The region is also within the world's largest irrigated agricultural area and has a dense population (Yao *et al.*, 2022). ~~As the GKLRJ is located in the transition belt between the TP's semi-arid and humid regions (Zheng *et al.*, 2010), it is seminal to the study of periglacial geomorphology.~~

Tectonically, the GKLRJ is located in the eastern part of the Ladakh-Kailas-Xiachayu magmatic arc of the Gangdise-Himalayan collisional orogen; from the Late Paleozoic to the Mesozoic, it has experienced the same evolutionary tectonic processes as the Gangdise-Himalayan archipelagic arc-basin systems, *i.e.*, back-arc spreading, arc-arc collision and arc-continental collision (Pan ~~*et al.*~~*et al.*, 2013). The GKLRJ's main rock types include Late Cretaceous quartz monzonite, Eocene monzonite and Eocene biotite granite. It is located in the transition belt between the TP's semi-arid and humid regions (Zheng *et al.*, 2010), m~~M~~ainly dominated by the Indian Summer Monsoon (ISM)~~,~~, T~~t~~he middle and western parts of the GKLRJ belong to the TP's temperate, semi-arid zone, while the eastern part belongs to plateau's temperate humid region (Zheng ~~*et al.*~~*et al.*, 2010). The mean annual air temperature (MAAT) is -7.2~~~~ ~~8.8ºC (Du and Yi, 2019), and the mean annual ground temperature (MAGT) is~~ ~~-3.2 ~~4.3ºC (Ran ~~*et al.*~~*et al.*, 2020). The mean annual precipitation (MAP) is 177 ~~-708 mm, decreasing from east to west across the study area (Du and Yi, 2019) (see Table.1). Changes in the imbalance between glaciers, permafrost, lakes and rivers in this region under the influence of climate change may lead to spatial and temporal changes in local ecosystems and changes in water resources in downstream areas (Yao *et al.*, 2022).

Table 1: MAAT (Du and Yi, 2019), MAGT (Ran *et al.*, 2020), MAP (Du and Yi, 2019), mean alititude(ASTER GDEM v3) and mean glacier ELA~~Topo-climatic~~(Liu *et al.*, 2012) ~~data~~ for the GKLRJ and its three sub-regions.

Region	MAAT (ºC)	MAGT (ºC)	MAP (mm)	Mean a~~A~~ltitude (m asl)	Mean glacier ELA (m asl)
All	0.69	0.53	469	4,623	5,431
R1	1.78	1.65	385	4,589	5,484
R2	-0.63	-0.06	489	4,893	5,462
R3	0.91	0.01	534	4,398	5,292

MAGT: mean annual ground temperature
MAAT: mean annual air temperature
MAP: mean annual precipitation

We divided the GKLRJ into three sub-regions: R1(east); R2 (central); and R3(west). These divisions were geospatially based (see Fig.1b), where R1 and R2 are bounded by the eastern marginal rift valley of the Oiga Basin, and R2 and R3 are bounded by Niang River, a tributary of the Niyang River. Each sub-region displays unique characteristics in terms of its topography and climate (see Table 1). The whole of R1 is a semi-arid region, and the terrain is more complex here. The western side of R1 is composed of a deep alpine valley landscape formed by glacial-fluvial erosion cutting through the undulating terrain, while the eastern side is a basin formed by ~~late~~ paleoglacial erosion and fluvial erosion cutting through less undulating mountainous hills with relatively gentle tops (Wu ~~*et al.*~~*et al.*, 2010). R2 is a semi-arid and semi-humid transition zone where the dividing line is located in its northeastern part; the mean altitude here is higher than in the other regions. The main peaks of glacier-carved mountains occur mostly above 5,500 m asl. R3 is located in a semi-humid zone where precipitation is more abundant and the terrain is on average ~~~~500 m lower than that of R2.

3 Material and methods

3.1 Rock glacier inventory, classification and database

We used high-resolution ©Google Earth Pro remote sensing images from ~~February~~ March ~~2009~~ 2004 to ~~December~~ August 2020 to manually and visually interpret and compile a rock glaciers inventory for the GKLRJ (Selley ~~*et al.*~~*et al.*, 2018; Magori ~~*et al.*~~*et al.*, 2020; Hassan ~~*et al.*~~*et al.*, 2021). The inventorying strategy follows the RGI_PCv2.0 (RGIK, 2022b). According to the technical definition of rock glaciers, we conducted the detection of rock glacier landforms in the study area and confirmed the relevant landforms (system/unit). For areas with missing clear imagery and those covered by snow, we simultaneously used the ©Map World for comparison and verification, ensuring that all outline segments can be labeled with certainty. Each cataloged rock glacier system/unit was assigned a primary ID and delineated according to the extended standards, with the outline encompassing the entire rock glacier up to the rooting zone, including its external parts such as the front and lateral margins (RGIK, 2022b). We followed as closely as possible the specific rules for delineating the upper boundaries of the rock glacier and provided information on their upslope connection type in the attribute table (RGIK, 2022a, 2022b). Due to the limited availability of accurate field observations and related data on rock glacier dynamics, their activity states were determined solely based on geomorphological criteria (RGIK, 2022a). The activity type of each rock glacier was recorded in the attribute table.

~~The identified rock glaciers were delineated from the rooting zone to the foot of the front slope in Google Earth Pro following the method used in previous studies (Scotti *et al.*, 2013; Jones *et al.*, 2021). The central point, length (parallel to flow) and width (vertical to flow) were also digitized in Google Earth Pro. We re-examined and adjusted the outlines of rock glaciers after the RGI_PCv2.0 (RGIK, 2022) update to ensure that they complied with the latest guidelines. Due to the lack of accurate field observations and related data on rock glacier dynamics, their activity states were determined according to the front slope, vegetation coverage, surface flow structures, rock glacier body and other geomorphic indicators. We divided rock glaciers into two types (intact/relict) according to the method used by Scotti *et al.* (2013). The active and inactive types were co-designated as 'intact rock glaciers' in this study (Haeberli, 1985; Pandey, 2019; Jones *et al.*, 2021). The intact rock glaciers usually have steep front slopes and lateral edges, an absence of vegetation cover, and apparent flow structures, such as ridges and furrows. The relict rock glaciers have relatively gentle frontal slopes, poorly defined lateral margins, a subdued topography, and less prominent flow structures (Scotti *et al.*, 2013; Baral *et al.*, 2019). Based on the sources of the sedimentary material, we divided these rock glaciers into four types: (A) intact debris-derived rock glaciers; (B) intact talus-derived rock glaciers; (C) relict debris-derived rock glaciers; and (D) relict talus-derived rock glaciers (see Fig. 2). The talus-derived rock glaciers are mostly located at the bottom of the talus slopes, and principally transport frost-shattered rock fragments derived from adjacent rock walls that have fallen under the force of gravity. The debris-derived rock glaciers are related to perennially frozen morainic material from older glacial advances mostly between the Holocene and the Little Ice Age (LIA), and mainly transport reworked glacial debris (till) (Barsch, 1996; Lilleøren and Etzelmüller, 2011; Scotti *et al.*, 2013).~~

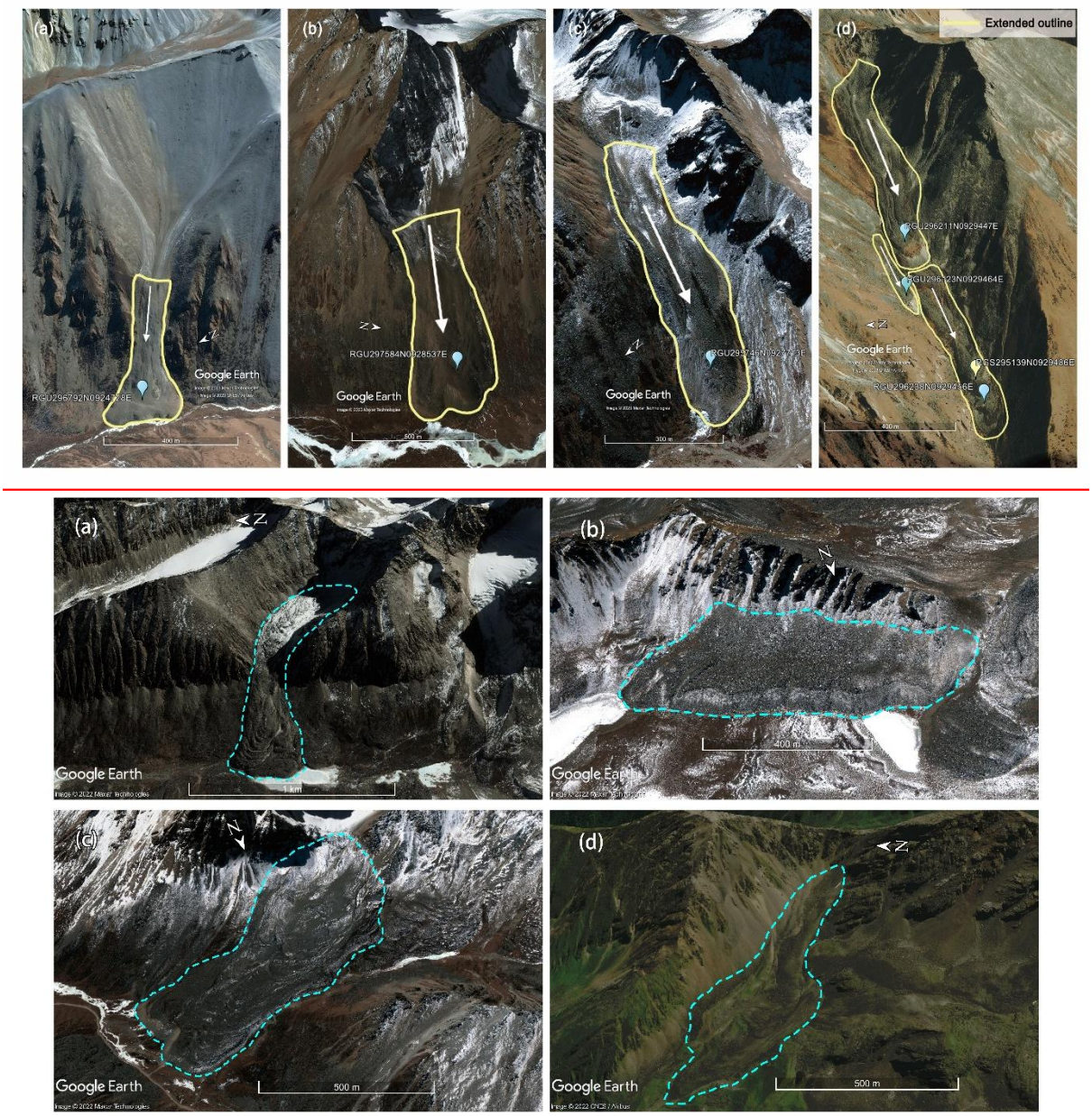

Figure 2: Example images of different upslope boundary types of rock glaciers in the GKLRJ. (a) a ~~An intact debris-derived~~deris-mantled slope-connected rock glacier; (b) a talus-connected ~~an intact talus-derived~~ rock glacier; (c) a glacier forefield-connected ~~relict debris-derived~~ rock glacier; (d) a ~~relict talus-derived~~ rock glacier system. Images from ©Google Earth.

All shapefiles were fed into the ~~1984 UTM~~WGS 1984 ~~Zone 46N~~ coordinate~~projection~~ system to extract their topographic attributes using ArcGIS 10.7 software. The parameters (i.e., latitude, longitude, area~~, length and width~~) of each rock glacier were calculated directly in ArcGIS ~~to further divide the geometric types according to their length-width ratios. Rock glaciers with a length/width ratio of < 1 were classified as lobate-shaped rock glaciers, while those with a length/width ratio of > 1 were classified as tongue-shaped rock glaciers (Baroni et al., 2004; Nyenhuis et al., 2005; Scotti et al., 2013)~~. Topographic data were derived from the Terra Advanced Spaceborne Thermal Emission and Reflection Radiometer Global Digital Elevation Model Version 3 (ASTER GDEM v3). We measured the mean altitude of each rock glacier, and quantified the mean slope and aspect of each rock glacier using the Surface tools in the ArcGIS Spatial Analyst toolbox. The aspect was primarily determined based on the majority result and adjusted in accordance with the actual slope direction. Each attribute was extracted using the ArcGIS Zonal Statistics tool. In, addition, the potential incoming solar

radiation (PISR) was calculated in SAGA 8.1.3 software. Analysis of variance (ANOVA) was used in ©SPSS 27 (IBM Corp, 2020) to analyse the differences in rock glacier metrics between groups.

Table 2: Certainty Index applied to each rock glacier (Jones et al., 2018b)

Parameter	Parameter options (index code)		
	1 point	2 points	3 points
External boundary	None (ON)	Vague (OV)	Clear (OC)
Snow coverage	Snow (SS)	Partial (SP)	None (SN)
Longitudinal flow structure	None (LN)	Vague (LV)	Clear (LC)
Transverse flow structure	None (TN)	Vague (TV)	Clear (TC)
Front slope	Unclear (FU)	Gentle (FG)	Steep (FS)
Certainty Index score	Medium certainty (MC) ⩽5	High certainty (HC) 6 to 10	Virtual certainty (VC) ⩾11

To reduce further the subjectivity associated with the identification, digitization and classification of landforms introduced by factors such as cloud cover, snowfall coverage and image quality in the inventory, we assessed the uncertainty for each rock glacier according to the method provided by Schmid *et al.* (2015), which has been widely used in previous studies (Jones *et al.*, 2018b; Brardinoni *et al.*, 2019; see Table 2). Most of the assessment work was finished in Google Earth Pro, and we rechecked the remote sensing image in Mapcarta (https://mapcarta.com/Map) when the rock glacier was covered by snow, and without other period imagery. Finally, we recorded the certainty index of each rock glacier in the attribute table (see Supplementary Materials).

3.2 Estimating hydrological stores

To calculate more accurately the water content (water volume equivalent, WVEQ [km^3]) of the perennially frozen rock glaciers (including active and transitional rock glaciers) and of surface ice in glaciersintact rock glaciers and clean ice glaciers in the GKLRJ (Jones *et al.*et al., 2018b), we chose two different methods derived from Brenning *et al.*et al. (2005a) and Cicoira *et al.*et al. (20202021).

The method for calculating the subsurface ice volumes of rock glaciers permafrost provided by Brenning *et al.*et al. (2005a) requires multiplying the mean thickness, surface area and ice content of each rock glacier as in Eq. (1), then converting them to the WVEQ by assuming an ice density conversion factor of 0.9 g cm^{-3} (≡900 kg m^{-3}) (Paterson, 1994; Jones *et al.*et al., 2018b), thus:

$$V_{RG} = \text{Area} * \text{Mean thickness} * \text{Ice Content} \quad (1)$$

Based on field data from Brenning *et al.*et al. (2005a) and a rule-of-thumb given by Barsch (1977ce) for the Swiss Alps, the rock glacier thickness was modeled empirically as Eq. (2), thus:

$$\text{Mean thickness [m]} = 50 * (\text{Area [km}^2\text{]})^{0.2} \quad (2)$$

The method provided by Cicoira *et al.*et al. (20202021), based on the analysis of a dataset of 28 rock

glaciers from the Alps (23) and the Andes (5), estimated rock glacier thickness using a perfectly plastic model arrived at by solving Eq. (4) for H, assuming a yield stress of τ = 92 kPa (taking the mean driving stress from the dataset as a given), thus:

$$H = \frac{\tau}{\rho\, g\, sin\alpha} \pm 3.4m \quad (3)$$

where τ is the sheer stress (τ= 92 kPa), g is the gravitational acceleration, H is the thickness of the moving rock glacier, α is the angle of the surface slope and ρ is the density of the creeping material, which is given by the contribution of volumetric debris w_d and ice content w_i and the relative densities (ρ_i = 910 kg m^{-3} and ρ_d = 2700 km m^{-3}), thus:

$$\rho = \rho_d\, w_d + \rho_i\, w_i \quad (4)$$

The ice content in rock glacier permafrost is spatially variable.~~Rock glaciers do not contain 100% ice by definition, and the ice content within them is spatially heterogeneous.~~ We therefore used global estimates of ice content within rock glacier to further calculate their lower (40%), mean (50%) and upper (60%) ice volumes (Hausmann ~~*et al.*~~*et al.*, 2012; Krainer and Ribis, 2012; Rangecroft ~~*et al.*~~*et al.*, 2015; Jones ~~*et al.*~~*et al.*, 2018b; Wagner ~~*et al.*~~*et al.*, 2021). In this study, the results of the calculations that used a 50% ice content were used for subsequent comparisons with ~~clean~~the surface ice in ~~ice~~ glaciers.

The ice volume of ~~clean ice~~ glacier was calculated using Eq. (5), thus:

$$V = A * H \ , \quad (5)$$

where V represents ice volume, A is the glacier surface area derived from the second Chinese glacier inventory (version 1.0) (2006-2011) (Liu ~~*et al.*~~*et al.*, 2012), and H is the ice thickness calculated using GlabTop2 in Python 3.10 (Linsbauer ~~*et al.*~~*et al.*, 2009). We assumed a 100% ice content by volume and applied the above ice density conversion factor to calculate the water equivalent volume of the ~~clean ice glaciers~~surface ice in glaciers.

To mitigate the additional impact caused by the uneven spatial distribution of glaciers and rock glaciers in the GKLRJ, we calculated a ratio of ~~intact~~ rock glaciers (including active and transitional rock glaciers)' to ~~clean ice~~ glaciers' water volume equivalence (WVEQ) by using the weighted average method that employs the following equation:

$$\text{WVEQ ratio}_{\text{Rg: Glacier}} = \frac{\text{WVEQ R1}_{\text{Rg}} \times \frac{\text{R1}_{\text{Rg}}}{\text{All}_{\text{Rg}}} + \text{WVEQ R2}_{\text{Rg}} \times \frac{\text{R2}_{\text{Rg}}}{\text{All}_{\text{Rg}}} + \text{WVEQ R3}_{\text{Rg}} \times \frac{\text{R3}_{\text{Rg}}}{\text{All}_{\text{Rg}}}}{\text{WVEQ R1}_{\text{Glacier}} \times \frac{\text{R1}_{\text{Glacier}}}{\text{All}_{\text{Glacier}}} + \text{WVEQ R2}_{\text{Glacier}} \times \frac{\text{R2}_{\text{Glacier}}}{\text{All}_{\text{Glacier}}} + \text{WVEQ R3}_{\text{Glacier}} \times \frac{\text{R3}_{\text{Glacier}}}{\text{All}_{\text{Glacier}}}} \quad (6)$$

where $\text{WVEQ ratio}_{\text{Rg: Glacier}}$ is the ratio of ~~intact~~ rock glaciers' to ~~clean ice~~ glaciers' WEVQ; $\text{WVEQ Rn}_{\text{Rg}}$ (n = 1, 2, 3) are the WVEQ values for rock glaciers in R1, R2 and R3, respectively; Rn_{Rg} (n = 1, 2, 3) are the numbers of rock glaciers in R1, R2 and R3, respectively; All_{Rg} is the number of rock glaciers in the whole GKLRJ; $\text{WVEQ Rn}_{\text{Glacier}}$ (n = 1, 2, 3) are the WVEQ values for ~~clean ice~~ glaciers in R1, R2 and R3, respectively; $\text{Rn}_{\text{Glacier}}$ (n = 1, 2, 3) are the number of ~~clean ice~~ glaciers in R1, R2 and R3, respectively; and $\text{All}_{\text{Glacier}}$ is the number of ~~clean ice glaciers~~glaciers in the whole GKLRJ.

~~3.3 Permafrost probability distribution~~

~~The binary logistic regression model has been used in several studies worldwide to calculate permafrost probability distribution (Sattler *et al.*, 2016; Deluigi *et al.*, 2017; Baral *et al.*, 2019; Hassan *et al.*, 2021). A logistic regression model can be formulated as Eq. (7), thus:~~

$$P(Y=1)=\frac{1}{1+e^{-(\beta_0+\sum\beta_n X_n)}} \quad (7)$$

where $P(Y=1)$ is the probability of outcome Y taking the value 1, β_0 is the intercept, and β_n is the regression coefficient of the independent variable X_n and is considered a predictor for the outcome Y. e is the base of the natural logarithm (Hassan *et al.*, 2021).

As viscous creep features in perennially frozen rock-ice mixtures, intact rock glaciers are considered to be direct expressions of permafrost. After calibrating the rock glacier inventory for the GKLRJ by taking activity state as the dependent variable, its intact and relict rock glaciers were taken to represent the occurrence (1) and non-occurrence (0) of permafrost, respectively. The spatially distributed local topo-climatic data (see Table 3), *i.e.*, longitude, latitude, mean altitude (ASTER GDEM v3), MAP in 2015 (Du and Yi, 2019), MAGT in 2015 (Du and Yi, 2019), mean slope and area (calculated in ArcGIS 10.7 based on ASTER GDEM v3) were used as the independent variables. All datasets were resampled to the same spatial resolution with the altitude data (~ 30 m) using the Nearest Neighbor method in ArcGIS 10.7 prior to analysis.

Table 3: Topo-climatic data information.

Factor	Year	Data source	Resolution
Latitude	/	Google Earth Pro	/
Longitude	/	Google Earth Pro	/
Area	/	ArcGIS 10.7	/
Mean altitude	2000-2013	ASTER GDEM v3	30 m
Slope	2000-2013	ASTER GDEM v3	30 m
MAGT	2005-2015	Ran *et al.*, 2019	1 km
MAP	2015	Du and Yi, 2019	1 km

MAGT: mean annual ground temperature
MAP: mean annual precipitation

We used the Forward Selection (Likelihood Ratio) method in SPSS 27.0 to stepwise select the topo-climatic variables for building the logistic regression model. The performance of the model was measured by calculating the area under the receiver operating characteristic (AUROC). A model providing excellent prediction has an AUROC higher than 0.9, a fair model has an AUROC between 0.7 and 0.9, and a model is considered poor if it has an AUROC lower than 0.7 (Swets, 1988; Marmion *et al.*, 2009).

4 Results

4.1 Rock glacier inventory analysis

~~4.1.1 Rock glacier types and their distribution~~

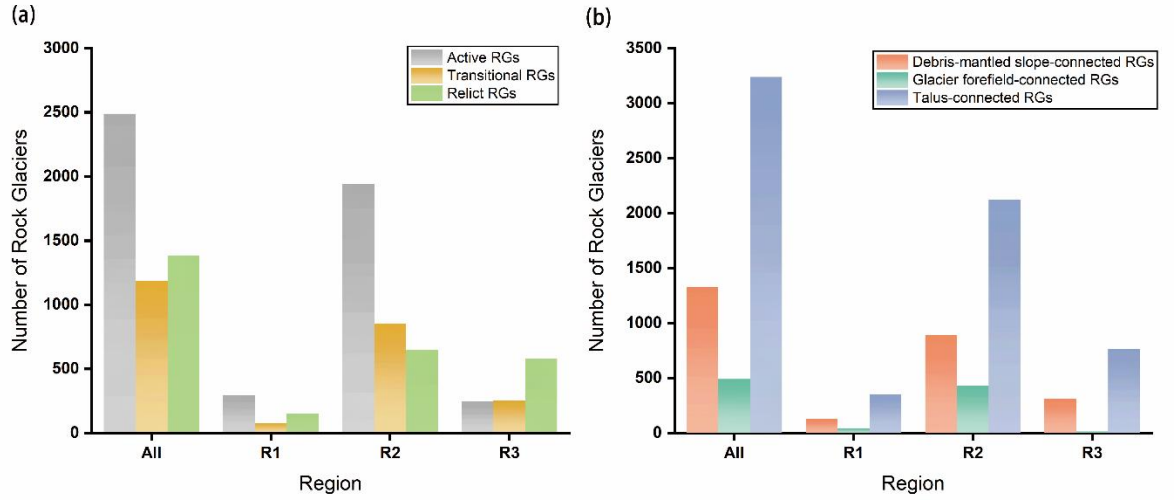

Figure 3: The number of rock glaciers categorized by different types of activity and upper slope connection in the entire GKRLJ and its sub-regions.

We identified a total of 5,057~~3~~ rock glaciers in the GKLRJ, including ~~830~~ 2,484 active~~intact debris~~ rock glaciers (~~16~~49.1%), 1,189 transitional~~3,548 intact talus~~ rock glaciers (23.5~~70~~%), 1,384~~68~~ relict ~~debris~~ rock glaciers (27.3~~1~~%) ~~and 607 relict talus rock glaciers (12%)~~. ~~~ 46% of the rock glaciers were classified as lobate-shaped, and ~ 54% as tongue-shaped. Talus-derived~~Active rock glaciers are predominant in the whole~~each region~~ GKLRJ, with the exception of R3 where a higher proportion of relict rock glaciers can be found (Fig. 3a). Among the total rock glaciers observed, ~64% of them (n = 3,239) were classified as talus-connected, ~26% (n = 1,327) as debris-mantled slope-connected, and ~10% (n = 491) as glacier forefield-connected, this order of proportions is consistent across three subregions. ~~However~~On the whole, rock glaciers are unevenly distributed in R1, R2 and R3, with nearly 70% of rock glaciers (n = 3,~~529~~447) distributed in R2 (see Table 4).

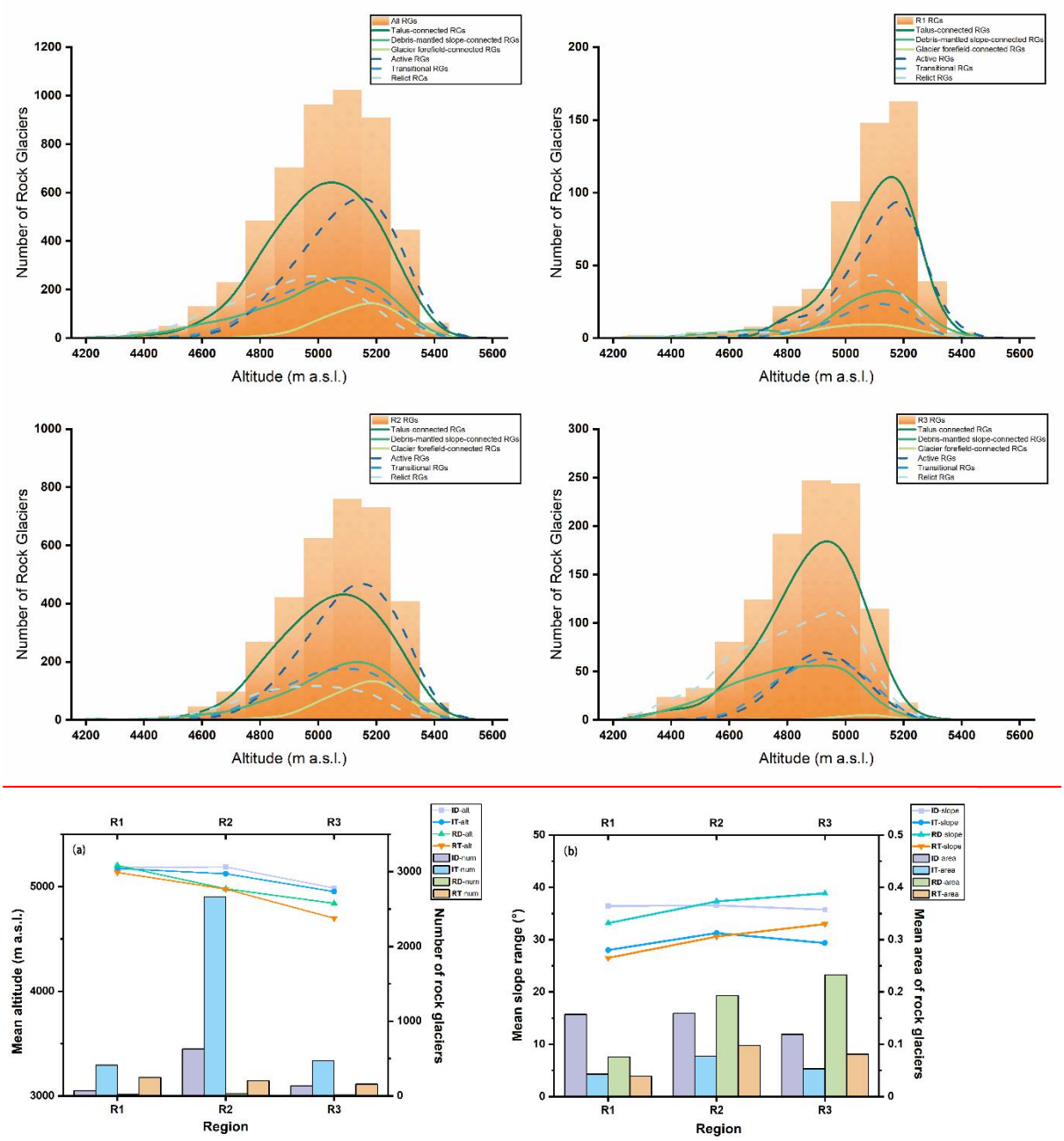

Figure ~~34~~: The mean occurrence altitude of rock glaciers categorized by different activity and upper slope connection types in (a)the whole GKLRJ and (b)R1, (c)R2 and (d)R3.
~~(a) Mean altitude and numbers of rock glaciers, by type; (b) mean range of slope and mean area of intact debris rock glaciers (ID), intact talus rock glaciers (IT), relict debris rock glaciers (RD) and relict talus rock glaciers (RT) in R1, R2 and R3.~~

~~~~~~90% of the rock glaciers are located between 4,800 and 5,400 m asl, with a mean altitude of ~~~5,~~123~~ 070 m asl. ~~Intact~~ Active rock glaciers are statistically distributed at higher altitudes than transitional and relict rock glaciers (ANOVA: F-value = 544.749, df within groups = 2, between groups = 5,054, p ≤ 0.001) ~~(ANOVA: *F*-value = 334.711, df within groups = 1, between groups = 5051, *p* ≤ 0.001)~~, at ~~~~140~~ 76 m and ~195 m higher. The mean alititude of rock glaciers varies significantly depending on the type of spatial connection to the upper slope (ANOVA: F-value = 102.9, df within groups = 2, between groups = 5,054, p ≤ 0.001). Compared to talus-connected (~5,063 m asl) and debris-mantled slope-connected rock glaciers (~5,044 m asl), glacier forefield-connected rock glaciers (~5,185 m asl) are more commonly found at higher elevations. The mean altitude of rock glaciers in R1 (~5,~~203~~ 132 m asl) is higher than for those in R2 (~5,~~189~~ 112 m asl)
~~~~~~

and R3 (~~4,~~987 909 m asl~~-~~) by ~~-~~40 20 m and ~~-~~250 223 m, respectively (see Table 4). The lower altitudinal limit of rock glaciers declines as longitude increases eastward (see Fig. 45).

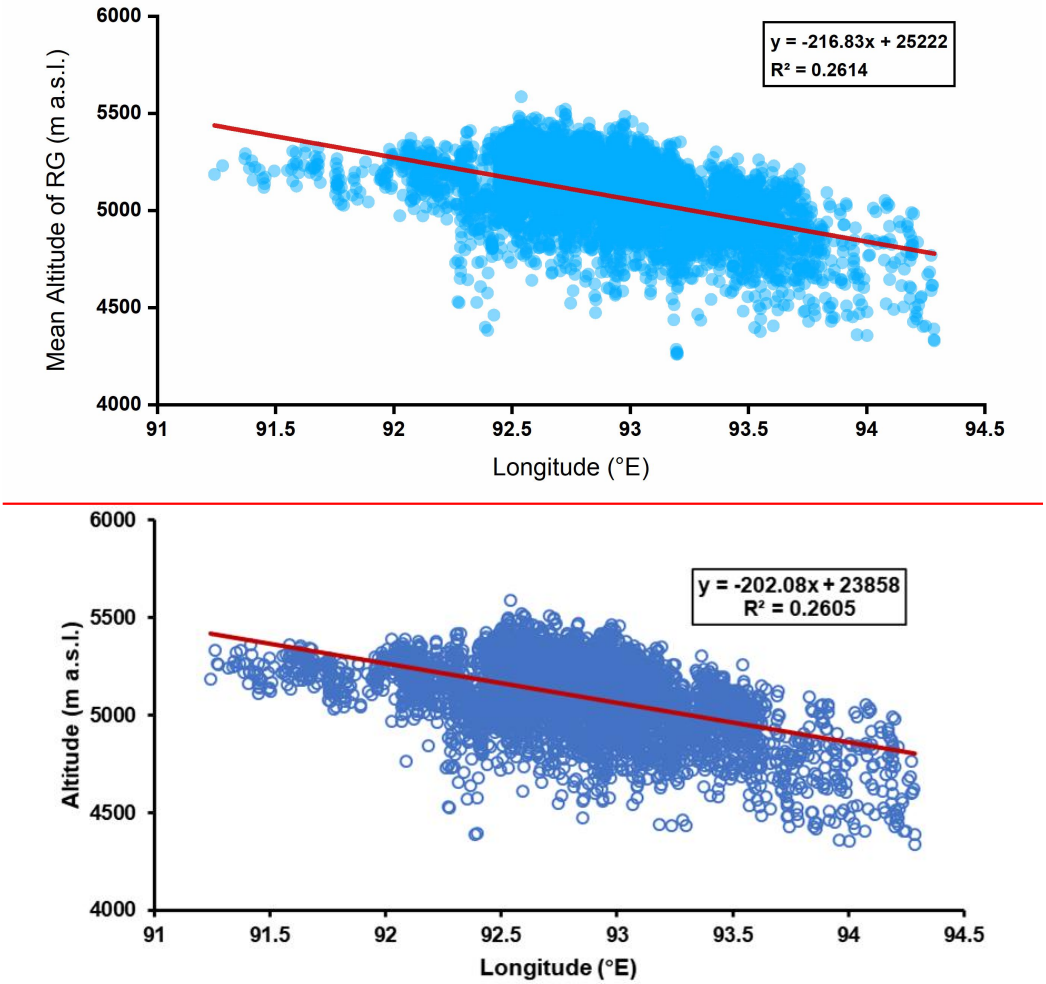

Figure 45: Scatterplots and fitted curves of the mean altitudinal distribution of rock glaciers *versus* longitude.

~~-~~In the GKLRJ, rock glaciers cover an area of ~~428~~404.~~697~~1 km^2, with the mean area of each rock glacier being 0.08 km^2~~,~~. the mena area of three different activity types of rock glaciers remains consistent with this value, but there are notable variations in the mean area of rock glaciers depending on their specific type of upper slope connection~~The different types of rock glaciers vary considerably with mean area~~ (ANOVA: *F*-value ~~-~~ = 89.814~~215.769~~, df within groups = 2~~3~~, between groups = 5,0~~54~~49, $p \leqslant$ 0.001). Glacier forefield-connected~~Debris-derived~~ rock glaciers (0.12~~5~~ km^2) generally have a larger mean area than the talus-connected ones (0.08 km^2) and the debris-mantled slope-connected~~talus-derived~~ ones (0.~~07~~ 06 km^2)~~., and relict debris rock glaciers have a larger mean area (0.16 km^2) than the other types.~~ The mean area of most types of rock glacier is the ~~highest~~ biggest in R2~~, except for relict debris rock glaciers, where it is~~and small~~est~~er than in R1~~3~~ (~~(Fig. 3~~Table.4). ~~-~~Furthermore, the mean slope range of rock glaciers in R3 is significantly steeper compared to that in R1 and R2 (ANOVA: *F*-value = 81.175, df within groups = 2, between groups = 4,680, $p \leqslant$ 0.001).

Table 4: Mean characteristics for rock glaciers.

Type	R1	R2	R3
Number	524	3,447	1,086
Mean altitude (m asl)	5,132	5,117	4,909
Mean MEF (m asl)	5,083	5,051	4,845
Mean area (km^3)	0.06	0.08	0.07

Mean slope range (°)	19.85	19.23	21.43
Mean MAGT (ºC)	-0.02	-0.6	-0.9
Mean MAAT (ºC)	-1.68	-1.94	-1.54
Mean MAP (mm)	343	392	495

MEF: minimum altitude at the rock glacier front
MAGT: mean annual ground temperature
MAAT: mean annual air temperature
MAP: mean annual precipitation

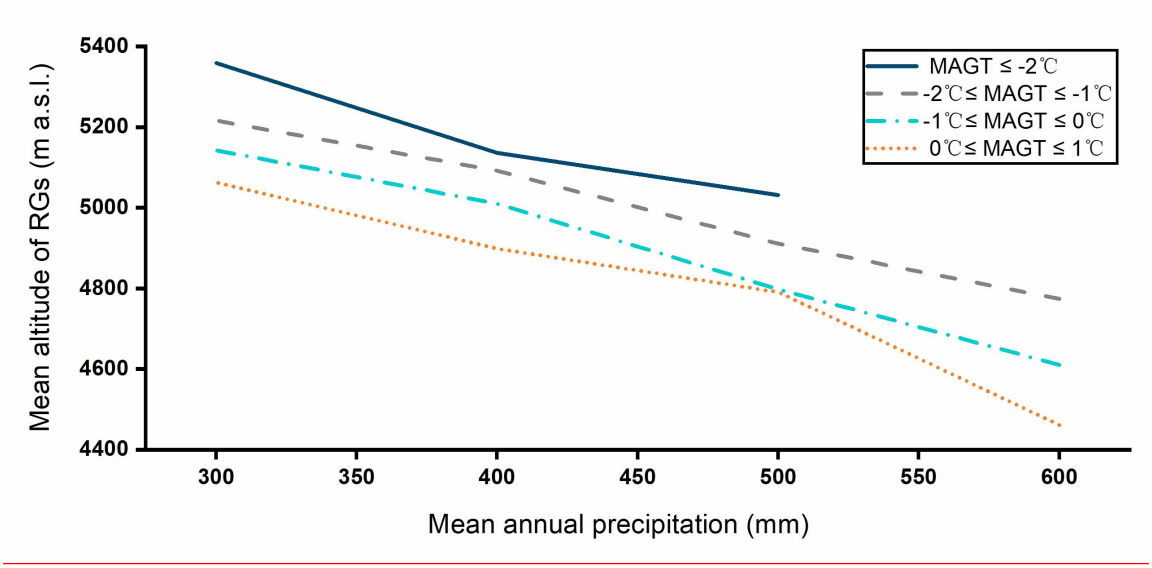

Figure 6: The variation in rock glacier distribution altitude with changes in precipitation for different MAGT states.

Around 90% of the rock glaciers in GKLRJ are found in the region where the MAGT ranges from -2°C to 0°C. Additionally, the MAGT, MAAT and MAP of the rock glaciers vary among the three sub-regions (Table.4). Specifically, the mean MAGT decreases gradually from R1 to R3, while the mean MAP increases gradually. The mean MAAT follows the same order as the regional mean MAAT values listed in Table 1. With the same MAGT, the mean altitude of rock glacier distribution decreases with increasing MAP. Moreover, with the same MAP, the altitude of rock glacier distribution increases with decreasing MAGT (Fig.6).

~~**Table 4: Mean characteristics for rock glaciers.**~~

~~Type~~	~~R1~~	~~R2~~	~~R3~~
~~Number~~	~~750~~	~~3,529~~	~~774~~
~~Mean altitude (m asl)~~	~~5,163~~	~~5,125~~	~~4,905~~
~~Mean MEF (m asl)~~	~~5,116~~	~~5,060~~	~~4,845~~
~~Mean area (km^3)~~	~~0.05~~	~~0.09~~	~~0.07~~
~~Mean slope range (º)~~	~~28.42~~	~~32.21~~	~~31.36~~
~~Mean MAGT (ºC)~~	~~-0.66~~	~~-0.60~~	~~-0.96~~
~~Mean MAAT (ºC)~~	~~-1.67~~	~~-1.96~~	~~-1.72~~
~~Mean MAP (mm)~~	~~339~~	~~390~~	~~502~~

~~MEF: minimum altitude at the glacier front~~
~~MAGT: mean annual ground temperature~~
~~MAAT: mean annual air temperature~~
~~MAP: mean annual precipitation~~

~~The mean range of surface slope of rock glaciers in the GKLRJ is ~ 30.46º; this value is larger than for R1 (28.42º), but smaller than for R2 (32.21º) and R3 (31.36º) (see Table 4). Moreover, debris-derived rock glaciers generally greater ranges in slope than talus-derived rock glaciers. The mean range of slope of the relict debris rock glaciers in R3 is the largest (38.87º) (Fig. 3).~~

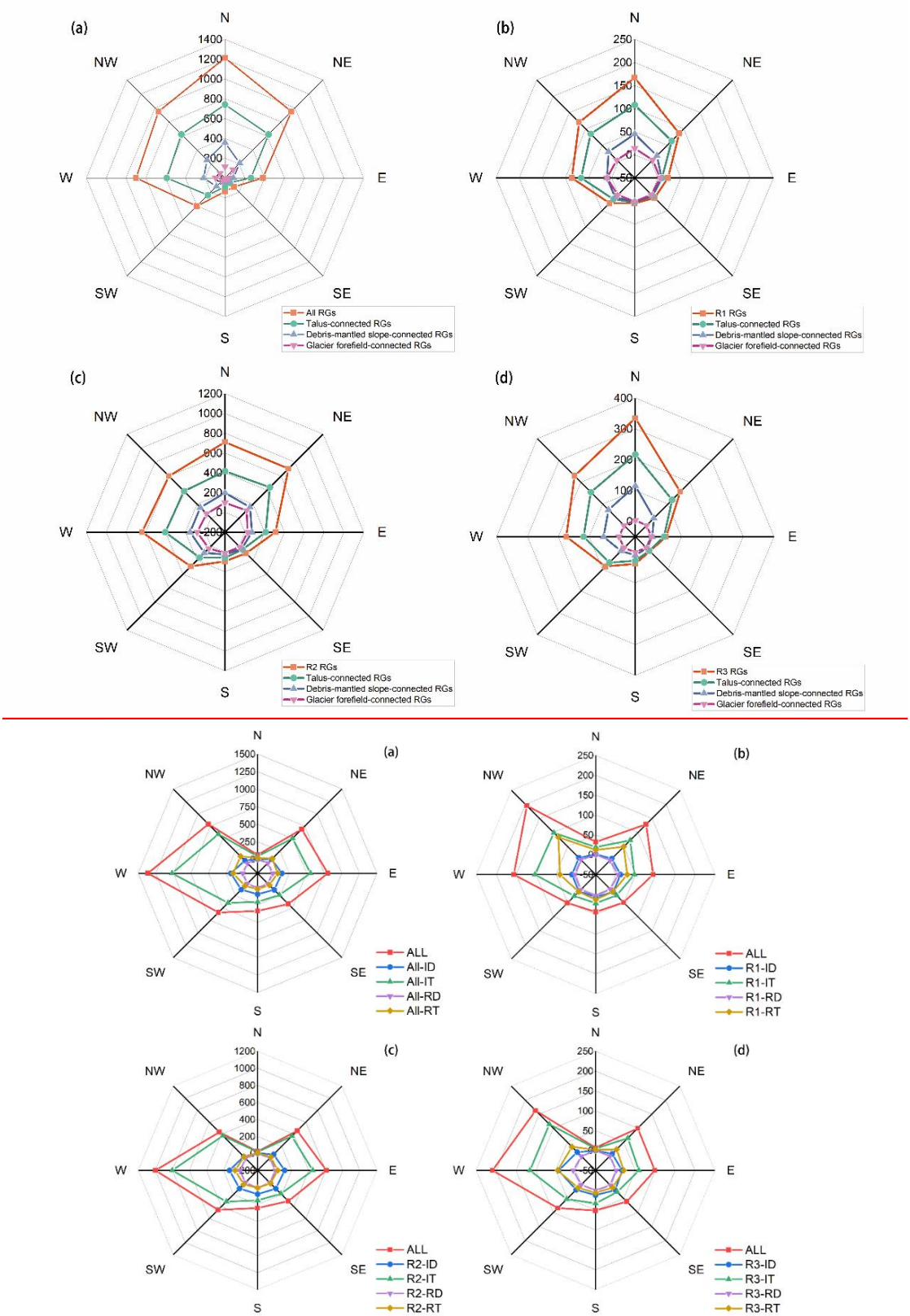

330 **Figure ~~5~~7: Analysis of abundances for different rock glacier activity states. The numbers of rock glaciers for each aspect on the four radar plots are shown as percentages (%). ~~Note: ID = intact debris-derived rock glacier; IT = intact talus-derived rock glacier; RD = relict debris-derived rock glacier; and RT = relict talus-derived rock glacier.~~**

~~———~~Rock glaciers predominantly occur on ~~west~~north-facing slopes (NW, 2~~3~~6.9~~7~~%; NW, ~~15.69~~18.7%; ~~SW~~NE, 1~~8.7~~8.7~~1.68~~%), with some distributed on the ~~east~~west-facing aspects (W, 17.7%~~E, 15.85%; NE, 13.62%~~),

335 and fewest on ~~north~~south-facing ~~slopes~~ aspects (S, 2.7~~1.23~~%; SE, 2.5%, SW, 7.9%) (see Fig. 5). ~~This is because~~

of the existence of numerous talus rock glaciers. Compared with the obvious characteristics of the concentrated distribution of rock glaciers in R1 and R3 on the N aspect, rock glaciers in R2 are more evenly distributed on the N, NE, W and NW aspects. The numbers of rock glaciers distributed on each aspect are consistent with those for the whole study area, although the proportion of rock glaciers distributed on west-facing slopes in R1 and R3 is larger than in R2.

4.1.2 Validation of the rock glacier inventory

Nearly 90% of rock glaciers in the GKLRJ have uncertainty indices concentrated between 9 and 12. Of these, the same number of rock glaciers with uncertainty 10 and 11 (n = 1,507) account for nearly 60% of the total number of rock glaciers. In general, the numbers of rock glaciers classified as 'high certainty' (n = 2,495) and 'virtual certainty' (n = 2,558) are similar, with a relatively even spatial distribution. Intact rock glaciers generally have a high certainty index, with all of them being 'virtual certainty'. Regionally, the main factors contributing to increased uncertainty vary between regions. The rock glaciers in R1 tend to be less clear in terms of their flow structure, while those in R2 and R3 are mainly influenced by snow coverage. Furthermore, the collapsed structures of the relict rock glaciers in R3 make their surfaces much more subdued than those of intact rock glaciers.

4.2 Water equivalent volumes

Based on the second Chinese glacier inventory (Liu *et al.et al.*, 2012), clean ice glaciersglaciers in the GKLRJ cover an area of ~~372.32 km^2. GlabTop2 provided estimated clean ice glacier thicknesses ranging between ~~1 and ~~263 m (mean = ~~18 m). We estimated the total WVEQ of the region's clean ice glaciersglaciers to be ~~9.29 km^3.

Table 5: Ice volumes (km^3) and corresponding WVEQs (km^3) calculated using the empirical area-thickness formula (Brenning, 2005a) for sub-regions and GKLRJ-wide (All).

Brenning, 2005a					
Region	Glacier - WVEQ (km^3)	RG - WVEQ (km^3)			RG: Glacier WVEQ ratio
		40%	50%	60%	
All	9.29	3.454.55	4.325.69	5.186.82	1:2.281:1.81
1	0.19	0.300.34	0.380.43	0.450.51	2:12.26:1
2	6.60	2.783.73	3.474.66	4.175.59	1:1.91:1.42
3	2.51	0.360.48	0.460.60	0.550.72	1:5.51:4.18

WVEQ = water volume equivalent

The mean ice thickness of intact rock glaciers in the GKLRJ estimated using the empirical area-thickness formula (Brenning, 2005a) is ~~28.48 35 m. The WVEQ storage lies between 4.553.45 and 5.186.82 km^3, of which R2 stores ~~80% of the water in the GKLRJ (*i.e.*, ~ 3.732.78 – 5.594.17 km^3). R1 stores 0.304 – ~0.51 45 km^3 of water (89% of the whole GKLRJ reserve). R3 stores ~~11% of the water, or 0.48 36 – 0.72 55 km^3(see Table 5). Compared to the WVEQ of clean ice glaciersglaciers, the result calculated using the weighted method showed that the ratio was 1:1.812.28, indicating that glaciers stored ~ 2.281.81 times more water than intact rock glaciers.

Table 6: Ice volumes (km^3) and corresponding WVEQs (km^3) calculated using the perfectly plastic model (Cicoira *et al.et al.*, 20210) for sub-regions and GKLRJ-wide (All).

Cicoira *et al.et al.*, 20210

Region	Glacier - WVEQ (km³)	RG - WVEQ (km³)			RG: Glacier WVEQ ratio
		40%	50%	60%	
All	9.29	1.31 – 2.021.93 – 2.85	1.64 – 2.532.71 – 3.86	1.97 – 3.043.69 – 5.07	1:4.661:3.20
1	0.19	0.11 – 0.170.16 – 0.23	0.14 – 0.220.22 – 0.31	0.17 – 0.260.30 – 0.41	1:1.061.42:1
2	6.60	1.08 – 1.651.54 – 2.29	1.35 – 2.062.16 – 3.09	1.62 – 2.482.94 – 4.06	1:3.861:2.51
3	2.51	0.11 – 0.190.24 – 0.34	0.14 – 0.240.34 – 0.46	0.17 – 0.290.45 – 0.61	1:13.211:6.28

WVEQ = water volume equivalent

The range of results in RG - WVEQ (km³) (Cicoira *et al.*et al., 20210) corresponds to $H \pm 3.4$ m.

The mean thickness of rock glaciers calculated using a perfectly plastic model (Cicoira *et al.*et al., 20210) is 19.1516.39±3.4 m, 9.3311.96 m thinner than that estimated using the empirical area-thickness formula. The mean value of the WVEQ estimated using this method is ~ 5641 – 6749% of the mean value obtained using the 'Brenning' method. As the estimated WVEQ of rock glaciers decreases, the ratio of rock glaciers' to clean-ice glaciersglaciers' WVEQ is also lower than that obtained using the 'Brenning' method (Brenning, 2005a), indicating that the WVEQ of clean-ice glaciersglaciers is ~~3.24.66 times that of rock glaciers (see Table 6).

4.3 Logistic regression modeling of permafrost probability distribution

Table 7: Selection of dependent variables for the logistic model.

	B	SE	*p*	Exp(B)	BCa 95% CI(B)	
					Lower	Upper
Mean altitude	0.007	0.000	0.000	1.008	1.007	1.008
Mean annual precipitation	-0.021	0.002	0.000	0.979	0.976	0.982
Mean slope	-0.041	0.009	0.000	0.960	0.943	0.977
Mean annual ground temperature	-0.145	0.073	0.047	0.865	0.750	0.998
Area	0.000	0.000	0.016	1.000	1.000	1.000
Longitude	4.327	0.215	0.000	75.742	49.659	115.524
Latitude	-2.320	0.275	0.000	0.098	0.057	0.168
Constant	-359.428	22.036	0.000	0.000		

We generated the estimation model based the logistic regression analysis result, all coefficient of variables included in the model were highly significant ($p < 0.05$, see Table 7). The Hosmer–Lemeshow test also showed that the model was a good fit ($p = 0.709$, $p > 0.05$). The area under the ROC curve (AUC) was calculated to be 0.85, which suggested that the model could be reliably used to predict the GKLRJ's permafrost probability distribution.

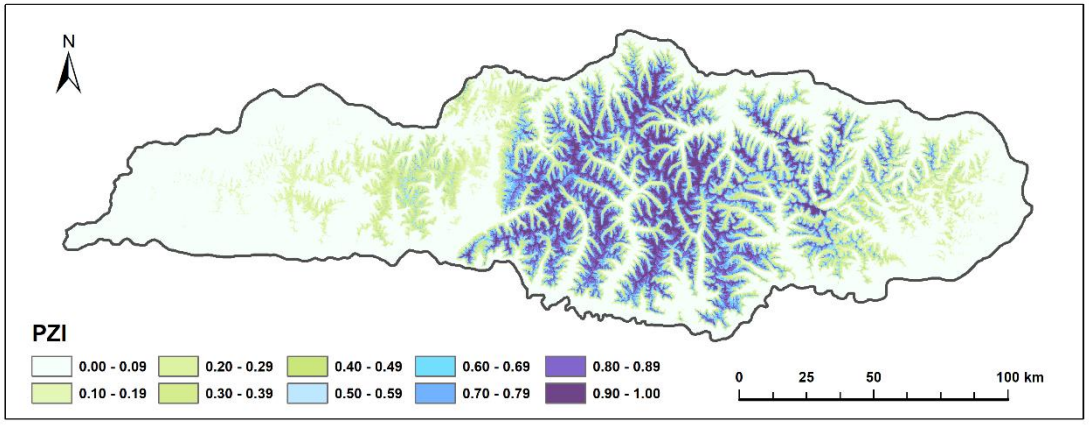

~~**Figure 6: Permafrost probability distribution map for the GKLRJ.**~~

~~Based on the above model, we drew a permafrost probability distribution map (Fig. 6). This map showed that ~ 30% of the GKLRJ (5,651 km^2) is in the PZI ≥ 0.5 permafrost probability zone. The maximum area (11,708 km^2; 51%) of the PZI occurs between the PZI values of 0.10 to 0.19, with a minimum altitude of 2,884 m asl, and close to the areas where MAGT = 0.5ºC and MAAT = 0ºC. The minimum altitude of permafrost probability areas with PZI values in the range of 0.50 ~ 0.59 is 4,476 m asl, where the MAGT is ~ 0ºC, close to the MAAT= -1ºC isotherm. The minimum altitude of permafrost probability areas with PZI values in the range of 0.89 ~ 0.99 is 4,790 ~ 5,860 m asl, where the MAGT is ~ -1.5ºC and the mean MAAT is ~ -3ºC, covering an area of 1,521 km^2 (6.6% of the total GKLRJ). As the minimum altitude of the PZI ≥ 0.5 areas is closest to the lower altitudinal limit of rock glaciers distributed in the GKLRJ (~ 4,500 m asl), we chose 0.5 as the critical value to classify the presence of permafrost in the GKLRJ. PZI ≥ 0.5 indicates that permafrost occurrence is probable, while PZI < 0.5 indicates that permafrost occurrence is improbable.~~

5 Discussion

5.1 Factors controlling rock glaciers

Rock glaciers are distributed heterogeneously throughout the GKRLJ, with most concentrated within R2. The GKLRJ spans a large area from east to west, with variations in topography and climatic conditions between the three sub-regions, thereby providing the basis for a spatially differentiated distribution of rock glaciers. The development of rock glaciers is a complex function of responses to air temperature, insolation, wind and seasonal precipitation over a considerable time period (Humlum, 1998), with the MAAT = -2°C isotherm and the equilibrium line altitude (ELA) for local glaciers forming the lower and upper boundaries of the cryogenic belt where they have developed, respectively (Humlum, 1988; Brenning, 2005a; Rangecroft ~~*et al.*~~*et al.*, 2015, 2016; Jones, 2018b). Topographically, the higher terrain in R2 has accommodated the development of more rock glaciers in the area above 4,500 m asl. R2 is located in the transition zone between the TP's semi-arid and sub-humid regions, with a mean ELA of ~~~~5,462 m asl. Compared with R3, which has a lower ELA (mean ELA = 5,292 m asl), and R1, which has a higher MAAT, R2 exhibits a broader range of the cryogenic belt to meet the development and distribution of more rock glaciers~~provides a large ecological niche for rock glacier development~~. Additionally, the widespread glacial remains in R2 and the predominance of more easily weathered granite as bedrock in this area could also provide a richer source of material for rock glacier

development (Wahrhaftig and Cox, 1959; Haeberli ~~*et al.*~~*et al.*, 2006).

———The mean and lower altitudinal limits of the rock glacier distribution in the GKLRJ decrease from west to east, from ~5,200 m asl to ~~~4,900 m asl. In the Gangdise Mountains, located in the same latitudinal range on the western side of the study area, rock glaciers show a similar trend of gradually decreasing altitude in line with increased moisture; indeed, the characteristics of the changes in the two regions show an overall continuity (Zhang ~~*et al.*~~*et al.*, 2022). Limited by the range of the ISM, MAP gradually decreases from west to east from the Gangdise Mountains to the GKLRJ. In the alpine tundra of this region, annual precipitation is dominated by snowfall in summer and autumn. Increases in snowfall in summer and autumn could help to preserve permafrost, allowing permafrost to develop at lower altitudes under similar climatic conditions (Zhou ~~*et al.*~~*et al.*, 2000). Additionally, annual regional precipitation values may reflect reductions in short-wave insolation arising from cloud cover, at least to some extent (Boeckli ~~*et al.*~~*et al.*, 2012a). Relatively favorable hydrological conditions will be more conducive to freeze-thaw weathering, thereby increasing the generation rate of rock debris, which in turn is conducive to the development of rock glaciers (Hallet ~~*et al.*~~*et al.*, 1991; Haeberli ~~*et al.*~~*et al.*, 2006; Zhang ~~*et al.*~~*et al.*, 2022). Increases in MAP are therefore likely to be conducive to the expansion of the range in the distribution of rock glaciers in semi-arid to sub-humid areas, meaning that the lower altitudinal limit of rock glacier distribution decreases with increases in annual precipitation.

Glacier forefield-connected rock glaciers may have a more abundant source of materials comparing to other types of rock glaciers. They distributed in regions where glaciers have previously existed, and both glacial moraines and surrounding rock walls can provide debris as their materials. Therefore, they have a more diverse range of material sources, which may contribute to the development of larger-scale rock glaciers. However, debris-mantled slope-connected rock glaciers lack significant headwall, and their debris is primarily produced by in-situ bedrock weathering (RGIK, 2022a). This results in their relatively limited and homogeneous material sources, leading to slower development and smaller scale compared to other types of rock glaciers.

———Rock glaciers in GKLRJ are primarily distributed on north-facing and west-facing aspects, which is remarkably similar to the distribution pattern of rock glaciers in the Himalayas (Jones *et al.*, 2018b), Gangdise Mountains (Zhang *et al.*, 2022), Tianshan Mountains (Liu *et al.*, 1995; Bolch and Marchenko, 2009) and the European Alps (Scotti *et al.*, 2013). This is mainly due to the fact that north-facing slopes receive less solar radiation as they are shaded, providing favorable conditions for the development and preservation of rock glaciers (Barsch, 1996). Additionally, the ample space and lower potential incoming solar radiation (PISR) on west-facing slopes, influenced by regional topographic conditions, also contribute to the development of rock glaciers here. This is evident in R2 where rock glaciers are more evenly distributed in the W, NW, N, and NE aspects compared to the distinct concentration of rock glaciers on the N aspect in R1 and R3.

~~**In the study area, rock glaciers are distributed mostly along west-facing aspects, followed by NW-facing slopes. This differs from the pattern in most regions where rock glaciers tend to be located on north-facing (NW-N-NE) mid-latitude mountains where solar radiation input is low, such as in the Himalayas (Jones *et al.*, 2018b), Gangdise Mountains (Zhang *et al.*, 2022), Tianshan Mountains (Liu *et al.*, 1995; Bolch and Marchenko, 2009) and the European Alps (Scotti *et al.*, 2013). However, regional topographic conditions appear to have a greater influence on the distribution of rock glaciers than solar radiation in the GKLRJ. The slopes here are predominantly east- and west-facing aspects, with north-facing aspects being lesson common in the region, and therefore unable to provide sufficient space**~~

~~for the distribution of rock glaciers. Therefore, rock glaciers within the GKLRJ are more commonly distributed on west-facing slopes, where the potential incoming solar radiation (PISR) calculated in SAGA 8.1.3 software is lower than for east-facing slopes.~~

~~Relict debris-derived rock glaciers exhibit a greater variation in slope within R2 and R3 compared to other types of rock glaciers. This is probably because R2 and R3 experience more intense freeze-thaw processes and more widespread glacial relics compared with R1, potentially providing a richer source of debris for rock glacier development. These debris-derived rock glaciers tend to be predominantly tongue-shaped (83%), with greater mobility and slope variation than talus-derived rock glaciers. Moreover, relict rock glaciers tend to be longer (681 m) compared to intact rock glaciers (616 m), another important factor in making their slopes more variable.~~

5.2 Hydrological significance of rock glaciers

In comparison, we found that the thicknesses of rock glaciers calculated using the flow plasticity model (Cicoira ~~*et al.*~~*et al.*, ~~2020~~2021) are significantly lower than the corresponding results calculated using the empirical area-thickness formula (Brenning, 2005a). By comparing the thickness of the rock glaciers calculated by both methods with the height of the rock glacier front measured in© Google Earth, the thickness of the rock glaciers calculated by the 'Cicoira' method (Cicoira *et al.*, 2021) seems to be closer to the real value. Therefore, we speculate that the thickness calculated based on the 'Brenning' method (Brenning, 2005a) may be overestimated to a certain extent due to the following reason. ~~, potentially due to the following three main reasons. First~~lyT~~, the angle of slope used to calculate the thickness may have been overestimated. Due to the lack of actual measurement data, we calculated the length of each rock glacier in ArcGIS based on the digitized results, extracted its altitudinal difference using DEM data, and finally applied trigonometric functions to calculate each angle of slope. Secondly, the angles of slope of some rock glaciers are outside the applicable slope range of this model (10°-30°). Since tongue-shaped rock glaciers on steep hillslopes tend to have steeper slopes and greater driving stresses, our estimates of thickness using the mean parameters in the model may be lower. Thirdly, t~~he applicability of different estimation methods may be different across the study area. The mean thickness of the sample rock glaciers in the study ~~made by~~of Brenning (2005a) about 30-50 m, which ~~is~~ are ~~~ 10 m~~ higher than the sample of rock glaciers selected in the study ~~conducted by~~of Cicoira ~~*et al.*~~*et al.* (~~2020~~2021) (15-30 m). We selected two rock glacier samples from Cicoira *et al.*'s (2021) research and used the 'Brenning' method (Brenning, 2005a) to calculate their thickness (Müller *et al.*, 2016). We observed that the calculated thickness (H=27 m) closely matched the actual thickness for the rock glacier with an area of 45,931 m^2 and a real thickness of 30 m. However, there was a significant discrepancy with the other rock glacier sample (H=25 m), which had an area of 32,356 m^2 and an actual thickness of 12 m. Therefore, the applicability of empirical formulaes based on various samples may vary for estimating the thickness of rock glaciers in different areas. As the thickness of rock glaciers in GKLRJ is relatively close to the sample selected by Cicoira *et al.* (2021), the application of the Brenning' method (Brenning, 2005a) may lead to an overestimation of rock glacier thickness in GKLRJ.~~ The thicknesses of rock glaciers estimated using Brenning's method may therefore be overestimates.~~

Based on the above discussion, we choose to use the results calculated based on the Cicoira' method

(Cicoira *et al.*, 2021), which may be closer to the actual water reserves in GKLRJ for further comparison and discussion~~. In order to facilitate comparison with the results of different studies worldwide, we chose to use the results obtained using the empirical area-thickness formula (Brenning, 2005a) for further discussion.~~ These estimates indicate that the amount of water stored in rock glaciers in the GKLRJ is ~~~~53.5% of the total previously-identified rock glacier water reserves globally (94.66 Gt), and ~~~~92.2% of the existing water reserves in rock glaciers on the TP (58.05 Gt) (Jones ~~*et al.*~~*et al.*, 2018a; Jones ~~*et al.*~~*et al.*, 2018b; Jones ~~*et al.*~~*et al.*, 2021). The rock glacier to glacier storage ratio in the GKJRJ of 1:~~1.82~~4.66 is ~~~~340~~ 133 times bigger than the global ratio (1:618, excluding the Antarctic and Subantarctic and Greenland Periphery Randolph Glacier Inventory) (Randolf Glacier Inventory (RGI); Pfeffer ~~*et al.*~~*et al.*, 2014; Jones ~~*et al.*~~*et al.*, 2018a), ~~~~5.414~~ times bigger than that of the Himalayas to its south (1:25) (Jones ~~*et al.*~~*et al.*, 2021), and much closer to that of the Andes in South America (1:3) (Azócar and Brenning, 2010), where glacier presence is also limited/absent ~~((Schrott, 1996;~~ Brenning, 2005b; Azócar and Brenning, 2010; ~~Millar and Westfall, 2019;~~ Jones ~~*et al.*~~*et al.*, 2019b; Schaffer ~~*et al.*~~*et al.*, 2019). In the GKLRJ, regional differences in the hydrological significance of rock glaciers under different climatic conditions also exist (ANOVA: F-value =~~5 8.263~~27.930, df within groups = ~~1.7732~~, between groups = ~~34.435~~3,671, $p \leqslant 0.001$). In R2, which is located in the transition zone between the semi-arid and semi-humid zones, the higher topography and suitable hydrothermal conditions lead to the highest concentration of glaciers and rock glaciers in this area, with rock glaciers accounting for 82% of the rock glacier water storage in the entire study area, and glaciers accounting for ~~73~~71% of the study area's glacial water storage, with a ratio of ~~~~1:~~1.42 3.86 between them. However, in terms of the ratio of rock glaciers to glacial water storage alone, rock glaciers are of greater hydrological significance in the warmer and drier R1, despite it storing only 8.7% of the total water volume of all rock glaciers~~, which has a storage capacity of only 7.6% of the total area~~. In the context of drought and climate warming, rock glaciers store more than twice the water of the glaciers in R1. This partly explains why rock glaciers have a greater hydrological significance and refuge potential as long-term reservoirs in arid regions with small and rapidly vanishing glaciers. Furthermore, the relationship between the proportion of the water cycle occupied by rock glaciers and the water requirements of regional populations should be considered in more detail. More research is needed into the hydrochemical composition of the stored water in rock glaciers and whether it can be used for irrigation and drinking.

5.3 Rock glaciers and permafrost presence ~~Rock glaciers can be used to model permafrost probability distribution~~

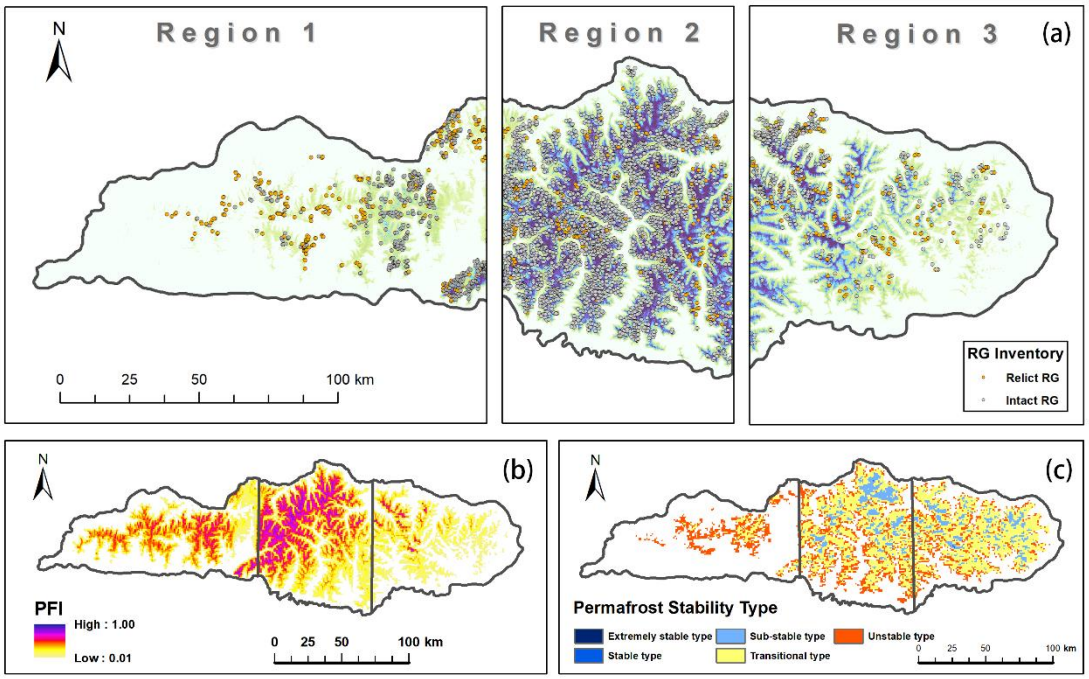

520

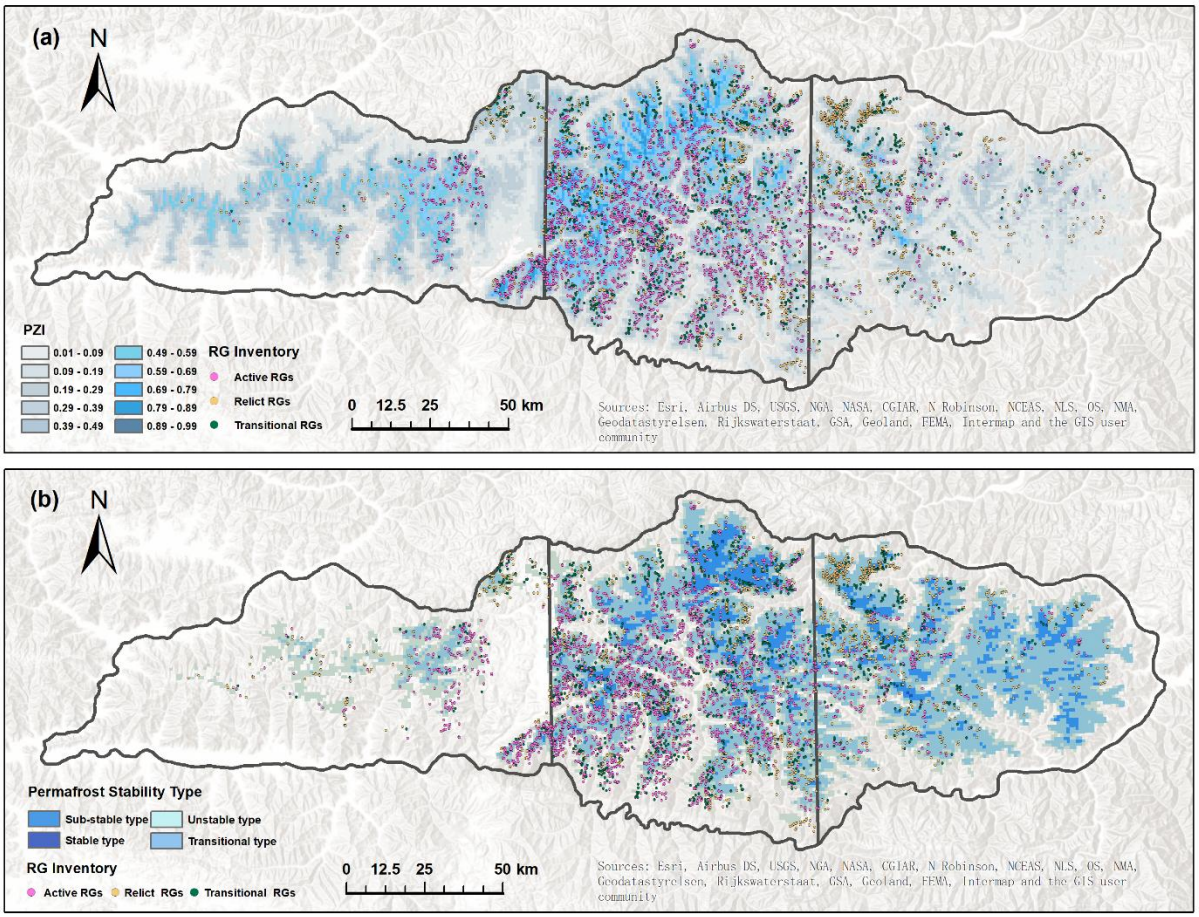

Figure ~~78~~: Spatial distribution of rock glaciers vs. (a) Gruber's (2012) Permafrost Zonation Index (PZI) in GKLRJ and (b) Map of the thermal stability of permafrost in GKLRJ (Ran *et al.*, 2020).

~~(a) Map of rock glaciers and permafrost probability distribution in the GKLRJ; (b) Gruber's (2012) Permafrost Zonation Index (PZI) for the GKLRJ; and (c) Map of the thermal stability of permafrost in the GKLRJ (Ran *et al.*, 2020).~~

The MAGT in GKLRJ is relatively high (Ran *et al.*, 2020; Ni *et al.*, 2020). Approximately 90% of the rock glaciers are distributed within the MAGT range of -2°C to 0°C, which belong to the regions of sub-stable type (−3°C < MAGT < −1.5°C), transitional type (−1.5°C < MAGT < −0.5°C), and unstable type permafrost (−0.5°C < MAGT < 0.5°C) (Cheng *et al.*, 2019). And about 7% of the rock glaciers occur in the seasonal frozen ground area with MAGT > 0°C. Overall, the distribution of rock glaciers in GKLRJ aligns well with the regions of Permafrost Zonation Index (PZI)≥0.49 in map provided by Gruber (2012) and the map of the thermal stability of permafrost provided by Ran *et al.* (2020), especially in R2 and the western part of R3. In R1, the range of permafrost distribution provided by Ran *et al.* (2020) is significantly smaller than the region with PZI ≥ 0.49 in Gruber (2012), while in the eastern part of R3 is larger. We speculate that these differences may be attributed to variations in the data period used in these studies. ~~The minimum altitude at the glacier front (MEF) of the intact rock glaciers (average = ~4,500 m asl) is close to the minimum altitude in the permafrost probability zone, with PZI > 0.50 (4,476 m asl), proving that the MEF of intact rock glaciers is a good indicator of permafrost distribution. Our predicted results are generally consistent with the PZI map (Gruber et al., 2012; Fig.7b) and the thermal stability of permafrost (Ran et al., 2020; Fig.7c), confirming that our rock glacier-based model has good applicability when simulating the distribution of permafrost in the GKLRJ.~~ When making detailed comparisons between the mean MAAT data from 1961 to 1990 used in the study of Gruber ~~et al.~~ (2012) and MAAT data for the TP in 2015 provided by Du and Yi (2019), we found that, except for a few areas in the eastern part of R3, the mean MAATs of R1 and R2 increased by ~~~2ºC. Although there may have been some errors in the data, the effect of temperature on the predicted permafrost distribution for the model based on the relationship between air temperature and the occurrence of permafrost may nonetheless be somewhat magnified. ~~These differences in the climate data' s reference time periods may have made our predicted range for R1significantly smaller than the range stated in Gruber *et al.* (2012). In R3, the permafrost probability distribution predicted by us is slightly lower than that of Ran *et al.* (2020), potentially related to the large number of relict rock glaciers in this area. Rock glaciers that extend so far from their source area, or into warmer climatic conditions at lower altitudes, may become inactive and evolve into relict rock glaciers. In these scenarios, the probability of permafrost occurrence in the region where the rock glaciers are located may be underestimated.~~

With future climate warming, the permafrost located in the eastern part of the Tibetan Plateau with lower ground temperatures may experience a faster warming rate (Cheng *et al.*, 2019). This could result in rapid changes in the movement speed and surface morphology of rock glaciers in GKLRJ over a short period of time (Krainer and Mostler, 2006; Ikeda *et al.*, 2008; Janke and Bolch, 2021). However, research has shown that despite the relatively rapid increase in ground temperatures in the deep layers of permafrost, the thawing of permafrost on the Tibetan Plateau occurs at a slow pace with full consideration of deep ground temperatures, subterranean ice and geothermal gradients in permafrost (Cheng *et al.*, 2019). It may take centuries, if not millennia, for the frozen material and corresponding subsurface ice in rock glaciers and permafrost to completely thaw and melt (Krainer *et al.*, 2015).

6 Conclusions

———We constructed an inventory of rock glaciers in the GKLRJ and illustrated their regional distribution characteristics and environmental indications. We employed two methods to estimate and compare the water storage capacity of the region's rock glaciers and map the GKLRJ's permafrost probability distribution using the logistic regression model. The results show that there are 5,053 057 rock glaciers in the GKLRJ, covering an area of 404.69428.71 km^2. Over 80% of these rock glaciers are located within R2,. Tand that the high altitude (~~4,900 m asl), low temperatures (MAAT ≤ -2ºC) and suitable precipitation (MAP ~~400 mm) in the semi-arid and semi-humid transition zone provide the greatest ecological nichewidest cryogenic belt range for rock glacier distribution in the region. The lower altitudinal limit of the distribution of rock glaciers decreases gradually with increasing longitude from the western side of the study area, from the Gangdise Mountains to the interior of the GKLRJ, indicating the positive effect of increased precipitation on the preservation of permafrost. We used two methods to estimate the thickness of rock glaciers and found that the results calculated based on the perfect plasticity model were more consistent with the actual situation in GKLRJ. Based on the empirical area-thickness formula estimation result, we calculated that 4.551.31 - -3.046.82 km^3 of water is stored in the rock glaciers, or ~~6133% of the water glaciers presently stored in surface ice of glaciers. The water volume estimated on the basis of the perfectly plastic model is 56-67% of this result. Despite these differences, both of these results reveal the previously neglected and important hydrological value of rock glaciers in the GKLRJ, particularly in R1, which is the drier sub-region. The WVEQ in rock glaciers and the ratio of subsurface ice in rock glacier permafrosts to surface ice in clean-ice glaciersglaciers may continue to increase with global warming and as glaciers retreat in the future. And the stability of permafrost in the area of rock glacier distribution is likely to further decline.The estimated results of our regression model are in good agreement with the predictions obtained using other methods and are also consistent with the actual distribution of rock glaciers. The lower altitude of the PZI ≥ 0.5 regions (~ 4,500 m asl) matches the boundary of the rock glacier distribution and the MAGT=0ºC isotherm, indicating that permafrost probably occurs. This also demonstrates that our predictive approach using the rock glacier inventory can better tackle the inherent interpretive problems caused by the region's complex topographic changes, as well as reflect more accurately the GKLRJ's current permafrost probability distribution.

Data availability. The data associated with this article can be found in the Supplementary Materials. These data include the Google maps of the most important areas described in this article, as well as a tabulation of the parameters of the rock glaciers found in the GKLRJ.

Author contributions. ML and GL designed the research. ML performed the analysis and wrote the paper. YY and ZP provided overall supervision and contributed to the writing.

Competing interests. The authors declare that they have no conflict of interest.

Acknowledgments. This work was supported by the Second Tibetan Plateau Scientific Expedition and

Research (STEP; Grant 299 no. 2019QZKK0205).

References

Alcalá-Reygosa, J.: Rock glaciers of the mountains of Mexico; a review of current knowledge and paleoclimatic implications, Journal of South American Earth Sciences, 96, 10.1016/j.jsames.2019.102321, 2019.

Arenson, L. U. and Jakob, M.: The Significance of Rock Glaciers in the Dry Andes - A Discussion of Azocar and Brenning (2010) and Brenning and Azocar (2010), Permafrost and Periglacial Processes, 21, 282-285, 10.1002/ppp.693, 2010.

Azocar, G. F. and Brenning, A.: Hydrological and Geomorphological Significance of Rock Glaciers in the Dry Andes, Chile (27 degrees-33 degrees S), Permafrost and Periglacial Processes, 21, 42-53, 10.1002/ppp.669, 2010.

Baral, P., Haq, M. A., and Yaragal, S.: Assessment of rock glaciers and permafrost distribution in Uttarakhand, India, Permafrost and Periglacial Processes, 31, 31-56, 10.1002/ppp.2008, 2019.

Baroni, C., Carton, A., and Seppi, R.: Distribution and behaviour of rock glaciers in the Adamello–Presanella Massif (Italian Alps), Permafrost and Periglacial Processes, 15, 243–259, https://doi.org/10.1002/ppp.497, 2004.

Barsch, D.: Eine A Eine Abschätzung von Schuttproduktion und Schutttransport im Bereich aktiver Blockgletscher der Schweizer Alpen. GéoProdig, portail d'information géographique, 28:148–160, 1977c.

Barsch, D.: Permafrost creep and rock glaciers, Permafrost and Periglacial Processes, 3, 175-188, https://doi.org/10.1002/ppp.3430030303, 1992.

Barsch, D.: Rockglaciers: Indicators for the Present and Former Geoecology in High Mountain Environments, Springer-Verlag, Berlin, pp. 331, 10.2307/3060377, 1996.

Berthling, I.: Beyond confusion: Rock glaciers as cryo-conditioned landforms, Geomorphology, 131, 98-106, 10.1016/j.geomorph.2011.05.002, 2011.

Blöthe, J. H., Rosenwinkel, S., Höser, T., and Korup, O.: Rock-glacier dams in High Asia, Earth Surface Processes and Landforms, 44, 808-824, 10.1002/esp.4532, 2019.

Boeckli, L., Brenning, A., Gruber, S., and Noetzli, J.: A statistical approach to modelling permafrost distribution in the European Alps or similar mountain ranges, The Cryosphere, 6, 125-140, 10.5194/tc-6-125-2012, 2012a.

Bolch, T. and Marchenko, S.: Significance of glaciers, rockglaciers and ice-rich permafrost in the Northern Tien Shan as water towers under climate change conditions, Selected Papers from the Workshop in Almaty, Kazakhstan, 2006, 8, 132–144, 2009.

Bolch, T., Rohrbach, N., Kutuzov, S., Robson, B. A., and Osmonov, A.: Occurrence, evolution and ice content of ice-debris complexes in the Ak-Shiirak, Central Tien Shan revealed by geophysical and remotely-sensed investigations, Earth Surface Processes and Landforms, 44, 129–143, https://doi.org/10.1002/esp.4487, 2019.

Bonnaventure, P. P. and Lamoureux, S. F.: The active layer: A conceptual review of monitoring, modelling techniques and changes in a warming climate, Progress in Physical Geography-Earth and Environment, 37, 352-376, 10.1177/0309133313478314, 2013.

~~Bosson, J.-B. and Lambiel, C.: Internal Structure and Current Evolution of Very Small Debris-Covered Glacier Systems Located in Alpine Permafrost Environments, Frontiers in Earth Science, 4, 10.3389/feart.2016.00039, 2016.~~

Brardinoni, F., Scotti, R., Sailer, R., and Mair, V.: Evaluating sources of uncertainty and variability in rock glacier inventories, Earth Surface Processes and Landforms, 44, 2450-2466, 10.1002/esp.4674, 2019.

Brenning, A.: Climatic and geomorphological controls of rock glaciers in the Andes of Central Chile: Combining Statistical Modelling and Field Mapping. Humboldt-Universität zu Berlin, Berlin, Germany, 2005a.

Brenning, A.: Geomorphological, hydrological and climatic significance of rock glaciers in the Andes of Central Chile (33-35 degrees S), Permafrost and Periglacial Processes, 16, 231-240, 10.1002/ppp.528, 2005b.

Buckel, J., Reinosch, E., Hördt, A., Zhang, F., Riedel, B., Gerke, M., Schwalb, A., and Mäusbacher, R.: Insights into a remote cryosphere: a multi-method approach to assess permafrost occurrence at the Qugaqie basin, western Nyainqêntanglha Range, Tibetan Plateau, The Cryosphere, 15, 149–168, https://doi.org/10.5194/tc-15-149-2021, 2021.

Cao, B., Li, X., Feng, M., and Zheng, D.: Quantifying Overestimated Permafrost Extent Driven by Rock Glacier Inventory, Geophysical Research Letters, 48, 10.1029/2021gl092476, 2021.

Cheng, G., Zhao, L., Li, R., Wu, X., Sheng, Y., Hu, G., Zou, D., Jin, H., Li, X., and Wu, B.: Characteristic, changes and impacts of permafrost on Qinghai-Tibet Plateau (in Chinese), Chinese Science Bulletin, 64, 2783-2795, 10.1360/TB-2019-0191, 2019.

Cicoira, A., Marcer, M., Gärtner-Roer, I., Bodin, X., Arenson, L. U., and Vieli, A.: A general theory of rock glacier creep based on in-situ and remote sensing observations, Permafrost and Periglacial Processes, 32, 139–153, https://doi.org/10.1002/ppp.2090, 2021.

Colucci, R. R., Boccali, C., Zebre, M., and Guglielmin, M.: Rock glaciers, protalus ramparts and pronival ramparts in the south-eastern Alps, Geomorphology, 269, 112-121, 10.1016/j.geomorph.2016.06.039, 2016.

Cui, P., Guo, X., Jiang, T., Zhang, G., and Jin, W.: Disaster Effect Induced by Asian Water Tower Change and Mitigation Strategies, Bulletin of the Chinese Academy of Sciences, 34, 1313-1321, 2019.

~~Deluigi, N., Lambiel, C., and Kanevski, M.: Data-driven mapping of the potential mountain permafrost distribution, Science of The Total Environment, 590–591, 370–380, https://doi.org/10.1016/j.scitotenv.2017.02.041, 2017.~~

Du, Y. Y., Yi, J. W.: Data of climatic factors of annual mean temperature in the Xizang (1990-2015), National Tibetan Plateau Data Center [data set], 2019.

Du, Y. Y., Yi, J. W.: Data set of annual rainfall and climate factors in Tibet (1990-2015), National Tibetan Plateau Data Center [data set], 2019.

Emmert, A. and Kneisel, C.: Internal structure of two alpine rock glaciers investigated by quasi-3-D electrical resistivity imaging, The Cryosphere, 11, 841–855, https://doi.org/10.5194/tc-11-841-2017, 2017.

French, H. M.: The Periglacial Environments (3rd Ed.), John Wiley & Sons Ltd, Chichester, UK, xviii + 458 pp, 2007.

Giardino, J. R. and Vitek, J. D.: The significance of rock glaciers in the glacial-periglacial landscape continuum, Journal of Quaternary Science, 3, 97-103, https://doi.org/10.1002/jqs.3390030111, 1988.

Gruber, S.: Derivation and analysis of a high-resolution estimate of global permafrost zonation, The Cryosphere, 6, 221-233, 10.5194/tc-6-221-2012, 2012.

Guo Z: Inventorying and spatial distribution of rock glaciers in the Yarlung Zangbo River Basin, Ph.D. thesis, Institute of International Rivers and Eco-Security, Yunnan University, China, 77pp., 2019.

Haeberli, W.: Creep of Mountain Permafrost: Internal Structure and Flow of Alpine Rock Glaciers, Mitteilungen der Versuchan-stalt fur Wasserbau, Hydrologie und Glaziologie (Zürich), 77, 1985.

Haeberli, W., Hallet, B., Arenson, L., Elconin, R., Humlum, O., Kääb, A., Kaufmann, V., Ladanyi, B., Matsuoka, N., Springman, S., and Mühll, D. V.: Permafrost creep and rock glacier dynamics, Permafrost and Periglacial Processes, 17, 189-214, https://doi.org/10.1002/ppp.561, 2006.

Halla, C., Blöthe, J. H., Tapia Baldis, C., Trombotto Liaudat, D., Hilbich, C., Hauck, C., and Schrott, L.: Ice content and interannual water storage changes of an active rock glacier in the dry Andes of Argentina, The Cryosphere, 15, 1187–1213, https://doi.org/10.5194/tc-15-1187-2021, 2021.

Hassan, J., Chen, X., Muhammad, S., and Bazai, N. A.: Rock glacier inventory, permafrost probability distribution modeling and associated hazards in the Hunza River Basin, Western Karakoram, Pakistan, Sci Total Environ, 782, 146833, 10.1016/j.scitotenv.2021.146833, 2021.

Hausmann, H., Krainer, K., Brueckl, E., and Ullrich, C.: Internal structure, ice content and dynamics of Ölgrube and Kaiserberg rock glaciers (Ötztal Alps, Austria) determined from geophysical surveys, Austrian Journal of Earth Sciences, 105, 12-31, 2012.

Humlum, O.: Rock Glacier Appearance Level and Rock Glacier Initiation Line Altitude: A Methodological Approach to the Study of Rock Glaciers, Arctic and alpine research, 20, 160-178, 10.2307/1551495, 1988.

Humlum, O.: The climatic significance of rock glaciers, Permafrost and Periglacial Processes, 9, 375-395, 10.1002/(sici)1099-1530(199810/12)9:4<375::Aid-ppp301>3.0.Co;2-0, 1998.

IBM Corp. IBM SPSS Statistics for Windows, Version 27.0, Armonk, New York, 2020.

Ikeda, A., Matsuoka, N., and Kääb, A.: Fast deformation of perennially frozen debris in a warm rock glacier in the Swiss Alps: An effect of liquid water, Journal of Geophysical Research: Earth Surface, 113, https://doi.org/10.1029/2007JF000859, 2008.

Janke, J., Bellisario, A., and Ferrando, F.: Classification of debris-covered glaciers and rock glaciers in the Andes of central Chile, Geomorphology-, 241, 98–121, https://doi.org/10.1016/j.geomorph.2015.03.034, 2015.

Janke, J. and Bolch, T.: Rock Glaciers. Reference Module in Earth Systems and Environmental Sciences, 2021.

Ji, J.Q., Zhong, D. L., Ding, L., Zhang, J.J., and Yang, Y. C.: Genesis and scientific significance of the Yarlung Zangbo Canvon, Earth Science Frontiers, 6, 231-235, 10.3321/j.issn:1005-2321.1999.04.005, 1999.

Jones, D. B., Harrison, S., Anderson, K., and Betts, R. A.: Mountain rock glaciers contain globally significant water stores, Scientific Reports, 8, 2834, 10.1038/s41598-018-21244-w, 2018a.

Jones, D. B., Harrison, S., Anderson, K., Selley, H. L., Wood, J. L., and Betts, R. A.: The distribution and hydrological significance of rock glaciers in the Nepalese Himalaya, Global and Planetary Change, 160, 123-142, 10.1016/j.gloplacha.2017.11.005, 2018b.

Jones, D. B., Harrison, S., Anderson, K., and Whalley, W. B.: Rock glaciers and mountain hydrology: A review, Earth-Science Reviews, 193, 66-90, 10.1016/j.earscirev.2019.04.001, 2019b.

Jones, D. B., Harrison, S., Anderson, K., Shannon, S., and Betts, R. A.: Rock glaciers represent hidden water stores in the Himalaya, Sci Total Environ, 793, 145368, 10.1016/j.scitotenv.2021.145368, 2021.

Kääb, A., Haeberli, W., and Gudmundsson, G. H.: Analysing the creep of mountain permafrost using high precision aerial photogrammetry: 25 years of monitoring Gruben Rock Glacier, Swiss Alps, Permafrost and Periglacial Processes, 8, 409-426, 10.1002/(sici)1099-1530(199710/12)8:4<409::Aid-ppp267>3.0.Co;2-c, 1997.

Krainer, K., Bressan, D., Dietre, B., Haas, J. N., Hajdas, I., Lang, K., Mair, V., Nickus, U., Reidl, D., Thies, H.,

and Tonidandel, D.: A 10,300-year-old permafrost core from the active rock glacier Lazaun, southern Ötztal Alps (South Tyrol, northern Italy), Quaternary Research, 83, 324–335, https://doi.org/10.1016/j.yqres.2014.12.005, 2015.

Krainer, K., and Mostler, W.: Reichenkar rock glacier: a glacier derived debris-ice system in the western Stubai Alps, Austria, Permafrost and Periglacial Processes, v. 11, no. 3, p. 267-275, 2000.

Krainer, K. and Ribis, M.: A rock glacier inventory of the Tyrolean alps (Austria), Austrian Journal of Earth Sciences, 105, 32–47, 2012.

Korup, O. and Montgomery, D. R.: Tibetan plateau river incision inhibited by glacial stabilization of the Tsangpo Gorge, Nature, 455, 786-U784, 10.1038/nature07322, 2008.

Lilleøren, K.S. and Etzelmüller, B.: A regional inventory of rock glaciers and ice-cored moraines in Norway, Geografiska Annaler: Series A, Physical Geography, 93, 175-191, https://doi.org/10.1111/j.1468-0459.2011.00430.x, 2011.

Linsbauer, A., Paul, F., Hoelzle, M., Frey, H., and Haeberli, W.: The Swiss Alps Without Glaciers - A GIS-based Modelling Approach for Reconstruction of Glacier Beds, https://doi.org/10.5167/uzh-27834, 2009.

Liu, G. N., Xiong, H. G., Cui, Z. J., and Song, C. Q.: The morphological features and environmental condition of rock glaciers in Tianshan mountains, Scientia Geographica Sinica, 15, 226-233, 297, 1995.

Liu, S., Guo, W., Xu, J.: The second glacier inventory dataset of China (version 1.0) (2006-2011). National Tibetan Plateau Data Center [data set], 10.3972/glacier.~~001.2013.db~~001. 2013.db, 2012.

Long, D., Li, X. Y., Li, X. D., Han, P. F., Zhao, F. Y., Hong, Z. K., Wang, Y. M., and Tian, F. Q.: Remote sensing retrieval of water storage changes and underlying climatic mechanisms over the Tibetan Plateau during the past two decades, Advances in Water Science, 33, 375-389, –10.14042/j.cnki.32.1309.2022.03.003, 2022.

Magori, B., Urdea, P., Onaca, A., and Ardelean, F.: Distribution and characteristics of rock glaciers in the Balkan Peninsula, Geografiska Annaler: Series A, Physical Geography, 102, 354-375, 10.1080/04353676.2020.1809905, 2020.

Mathys, T., Hilbich, C., Arenson, L. U., Wainstein, P. A., and Hauck, C.: Towards accurate quantification of ice content in permafrost of the Central Andes – Part 2: An upscaling strategy of geophysical measurements to the catchment scale at two study sites, The Cryosphere, 16, 2595–2615, https://doi.org/10.5194/tc-16-2595-2022, 2022.

Millar, C. I. and Westfall, R. D.: Rock glaciers and related periglacial landforms in the Sierra Nevada, CA, USA; inventory, distribution and climatic relationships, Quaternary International, 188, 90-104, 10.1016/j.quaint.2007.06.004, 2008.

Millar, C. I., Westfall, R. D., and Delany, D. L.: Thermal and hydrologic attributes of rock glaciers and periglacial talus landforms: Sierra Nevada, California, USA, Quaternary International, 310, 169-180, 10.1016/j.quaint.2012.07.019, 2013.

~~Millar, C. I. and Westfall, R. D.: Geographic, hydrological, and climatic significance of rock glaciers in the Great Basin, USA, Arctic, Antarctic, and Alpine Research, 51, 232–249, https://doi.org/10.1080/15230430.2019.1618666, 2019.~~Müller, J., Vieli, A., and Gärtner-Roer, I.: Rock glaciers on the run – understanding rock glacier landform evolution and recent changes from numerical flow modeling, The Cryosphere, 10, 2865–2886, https://doi.org/10.5194/tc-10-2865-2016, 2016.

Ni, J., Wu, T., Zhu, X., Hu, G., Zou, D., Wu, X., Li, R., Xie, C., Qiao, Y., Pang, Q., Hao, J., and Yang, C.: Simulation of the Present and Future Projection of Permafrost on the Qinghai-Tibet Plateau with Statistical and Machine Learning Models, Journal of Geophysical Research: Atmospheres, 126, e2020JD033402, https://doi.org/10.1029/2020JD033402, 2021.

Nyenhuis, M., Hoelzle, M., and Dikau, R.: Rock glacier mapping and permafrost distribution modelling in the Turtmanntal, Valais, Switzerland, Zeitschrift fur Geomorphologie, 49, 275–292, 2005.

Pan, G. T., Wang, L. Q., Zhang, W. P., Wang, B. D.: Tectonic Map and Specification of Qinghai Tibet Plateau and Its Adjacent Areas (1: 1 500 000), Geology Press, Beijing, 208pp, 2013.

Pandey, P.: Inventory of rock glaciers in Himachal Himalaya, India using high-resolution Google Earth imagery, Geomorphology, 340, 103-115, 10.1016/j.geomorph.2019.05.001, 2019.

Paterson, W. S. B.: The Physics of Glaciers, Butterworth-Heinemann, Oxford, 480pp, 1994.

Pfeffer, W. T., Arendt, A. A., Bliss, A., Bolch, T., Cogley, J. G., Gardner, A. S., Hagen, J. O., Hock, R., Kaser, G., Kienholz, C., Miles, E. S., Moholdt, G., Mölg, N., Paul, F., Radic, V., Rastner, P., Raup, B. H., Rich, J., and Sharp, M. J.: The Randolph Glacier inventory: a globally complete inventory of glaciers, Journal of Glaciology, 60, 537-552, 2014.

Ran, Y., Li, X., Cheng, G., Nan, Z., Che, J., Sheng, Y., Wu, Q., Jin, H., Luo, D., Tang, Z., and Wu, X.: Mapping the permafrost stability on the Tibetan Plateau for 2005–2015, Science China Earth Sciences, 64, 62-79, 10.1007/s11430-020-9685-3, 2020.

Ran, Z. and Liu, G.: Rock glaciers in Daxue Shan, south-eastern Tibetan Plateau: an inventory, their distribution, and their environmental controls, The Cryosphere, 12, 2327-2340, 10.5194/tc-12-2327-2018, 2018.

Rangecroft, S., Harrison, S., and Anderson, K.: Rock glaciers as water stores in the Bolivian Andes: an assessment of their hydrological importance, Arctic Antarctic and Alpine Research, 47, 89-98, 10.1657/aaar0014-029, 2015.

Rangecroft, S., Suggitt, A. J., Anderson, K., and Harrison, S.: Future climate warming and changes to mountain permafrost in the Bolivian Andes, Clim Change, 137, 231-243, 10.1007/s10584-016-1655-8, 2016.

Reinosch, E., Gerke, M., Riedel, B., Schwalb, A., Ye, Q., and Buckel, J.: Rock glacier inventory of the western Nyainqêntanglha Range, Tibetan Plateau, supported by InSAR time series and automated classification, Permafrost and Periglacial Processes, 32, 657-672, 10.1002/ppp.2117, 2021.

RGIK. Towards standard guidelines for inventorying rock glaciers: baseline concepts (version 4.2.2). IPA Action Group Rock glacier inventories and kinematics, 13 pp, 2022a.~~RGIK. Towards standard guidelines for inventorying rock glaciers: baseline concepts (version 4.2), IPA Action Group Rock glacier inventories and kinematics (Ed.), 13pp, 2021.~~

RGIK. Towards standard guidelines for inventorying rock glaciers: practical concepts (version 2.0). IPA Action Group Rock glacier inventories and kinematics, 10 pp. 2022b.

Sattler, K., Anderson, B., Mackintosh, A., Norton, K., and de Róiste, M.: Estimating Permafrost Distribution in the Maritime Southern Alps, New Zealand, Based on Climatic Conditions at Rock Glacier Sites, Frontiers in Earth Science, 4, 10.3389/feart.2016.00004, 2016.

Schaffer, N., MacDonell, S., Réveillet, M., Yáñez, E., and Valois, R.: Rock glaciers as a water resource in a changing climate in the semiarid Chilean Andes, Regional Environmental Change, 19, 1263-1279,

10.1007/s10113-018-01459-3, 2019.

Schmid, M. O., Baral, P., Gruber, S., Shahi, S., Shrestha, T., Stumm, D., and Wester, P.: Assessment of permafrost distribution maps in the Hindu Kush Himalayan region using rock glaciers mapped in Google Earth, Cryosphere, 9, 2089-2099, 10.5194/tc-9-2089-2015, 2015.

Schrott, L.: Some geomorphological-hydrological aspects of rock glaciers in the Andes (San Juan, Argentina), Zeitschrift fur Geomorphologie, Supplementband, 104, 161–173, 1996.

Schoeneich, P., Bodin, X., Echelard, T., Kaufmann, V., Kellerer-Pirklbauer, A., Krysiecki, J.-M., and Lieb, G. K.: Velocity Changes of Rock Glaciers and Induced Hazards, in: Engineering Geology for Society and Territory - Volume 1, Cham, 223–227, 2015.

Scotti, R., Brardinoni, F., Alberti, S., Frattini, P., and Crosta, G. B.: A regional inventory of rock glaciers and protalus ramparts in the central Italian Alps, Geomorphology, 186, 136-149, 10.1016/j.geomorph.2012.12.028, 2013.

Selley, H., Harrison, S., Glasser, N., Wündrich, O., Colson, D., and Hubbard, A.: Rock glaciers in central Patagonia, Geografiska Annaler: Series A, Physical Geography, 101, 1-15, 10.1080/04353676.2018.1525683, 2018.

Wagner, T., Kainz, S., Helfricht, K., Fischer, A., Avian, M., Krainer, K., and Winkler, G.: Assessment of liquid and solid water storage in rock glaciers versus glacier ice in the Austrian Alps, SCIENCE OF THE TOTAL ENVIRONMENT, 800, https://doi.org/10.1016/j.scitotenv.2021.149593, 2021.

Wahrhaftig, C. and Cox, A.: Rock glaciers in the Alaska Range, GSA Bulletin, 70, 383-436, 10.1130/0016-7606(1959)70[383:Rgitar]2.0.Co;2, 1959.

Xiang, S. Y.: 1:3 million Quaternary geological and geomorphological map of the Tibetan Plateau and its surrounding areas, China University of Geosciences Press, Wuhan, 104pp, 2013.

Yao, T., Wu, G., Xu, B., Wang, W., Gao, J., and An, B.: Asian Water Tower Change and Its Impacts, Bulletin of the Chinese Academy of Sciences, 34, 1203-1209, 2019.

Yao, T., Bolch, T., Chen, D., Gao, J., Immerzeel, W., Piao, S., Su, F., Thompson, L., Wada, Y., Wang, L., Wang, T., Wu, G., Xu, B., Yang, W., Zhang, G., and Zhao, P.: The imbalance of the Asian water tower, Nature Reviews Earth & Environment, 3, 618–632, https://doi.org/10.1038/s43017-022-00299-4, 2022.

Yu, X., Ji, J., Gong, J., Sun, D., Qing, J., Wang, L., Zhong, D., and Zhang, Z.: Evidence of rapid erosion driven by climate in the Yarlung Zangbo (Tsangpo) Great Canyon, the eastern Himalayan syntaxis, Chinese Science Bulletin, 56, 1123-1130, 10.1007/s11434-011-4419-x, 2011.

Zhang, Q., Jia, N., Xu, H., Yi, C., Wang, N., and Zhang, L.: Rock glaciers in the Gangdise Mountains, southern Tibetan Plateau: Morphology and controlling factors, CATENA, 218, 106561, https://doi.org/10.1016/j.catena.2022.106561, 2022.

Zheng J, Yin Y, Li B. A New Scheme for Climate Regionalization in China, ACTA GEOGRAPHICA SINICA, 65, 3-12, 10.11821/xb201001002, 2010.

Zhou Y, Guo D, Qiu G, Cheng G, Li S. Geocryology In China, Science Press, Beijing, 450pp, 2000.